

# ACCURACY ASPECT OF DTM USING SATTELITE PHOTOGRAMMETRY

## A DISSERTATION

*Submitted in partial fulfillment of the  
requirements for the award of the degree*

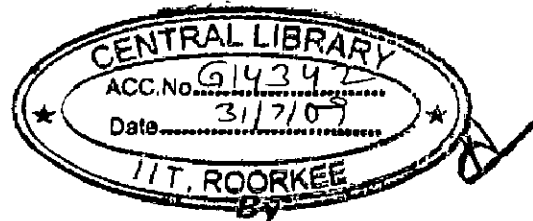
*of*

MASTER OF TECHNOLOGY

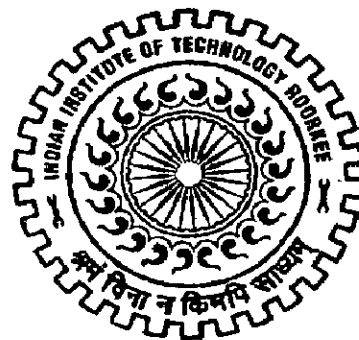
*in*

CIVIL ENGINEERING

(With Specialization in Geomatics Engineering)



**JITENDRA KUMAR AGRWAL**



GEOMATICS ENGINEERING GROUP  
DEPARTMENT OF CIVIL ENGINEERING  
INDIAN INSTITUTE OF TECHNOLOGY ROORKEE  
ROORKEE - 247 667 (INDIA)

JUNE, 2008

## **CANDIDATE'S DECLARATION**

---

I hereby declare that the work which is being presented in the dissertation entitled **“ACCURACY ASCEPTS OF DTM USING SATTELITE PHOTOGRAMMETRY”** in partial fulfilment of the requirements for the award of degree of **Master of Technology in Civil Engineering** with specialisation in **Geomatics Engineering**, submitted in the department of Civil Engineering, **Indian Institute of Technology Roorkee**, Roorkee is an authentic record of my own work carried out from December, 2007 to June, 2008 under the guidance of **Dr. Kamal Jain**, Assistant Professor, Geomatics Engineering Group, Department of Civil Engineering, Indian Institute of Technology Roorkee, Roorkee.

The matter embodied in this dissertation has not been submitted by me for award of any other degree or diploma.

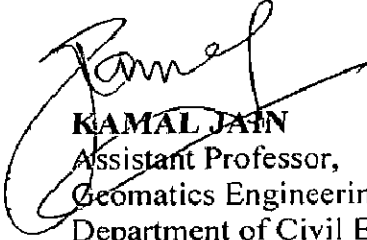
Roorkee

Dated: 30 June, 2008

  
(Jitendra Kumar Agrwal)

## **CERTIFICATE**

This is to certify that the above statement made by the candidate is correct to the best of my knowledge.

  
**KAMAL JAIN**  
Assistant Professor,  
Geomatics Engineering Group,  
Department of Civil Engineering,  
Indian Institute of Technology Roorkee,  
Roorkee-247667(UK) India

## ACKNOWLEDGEMENT

---


I wish to express my deep sense of gratitude to **Dr. Kamal Jain**, Assistant Professor, Geomatics Engineering Group, Department of Civil Engineering, Indian Institute of Technology Roorkee, Roorkee for his excellent guidance, generous help, constant encouragement and the time he spared for supervising this work. I also wish to express my sincere thanks to the entire faculty of Geomatics Engineering Group for extending all the help possible to me.

My sincere thanks to Mr. Mandla Ravi Babu, Mr. shashi m., Ms poonam Negi Research Scholar, Geomatics Engineering Group for the help they rendered in collection of extensive field data as well full support during this thesis.

I also wish to express my profound gratitude to all my family members and well wishers for the faith imposed in me and without whose patience and blessings this thesis would not have reached its present form.

A word of thanks also goes out to all my friends who have provided valuable suggestions and inputs during the various phases of my work.

Dated: 30 June, 2008

  
(Jitendra Kumar Agrwal)

## ABSTRACT

---

Photogrammetric approach to generate DTM has recently considerable interest in the remote sensing community for its simplicity and accuracy, especially in light of the trend that some commercial high resolution satellite imagery data are supplied with RPC without disclosing the physical sensor model.

RPC with stereo pair , provide full photogrammetric processing including 3-D reconstruction, DEM generation, orthorectification, block adjustment and feature extraction . This steady present a complete methodology for DEM generation from stereo satellite images using rational polynomial coefficient of the imagery geometry and comparative study between commercial software's accuracy and performance are checked for DEM generated from stereo image using RPC approach.

This study carried out the generation of DTM using RPC with different software and then compares these results. This study also consider factor affecting accuracy of DEM in the photogrammetric software. Like tie point generation process what parameter is passed and how they affect the accuracy of DEM.

# CONTENTS

---

<b>Title</b>	<b>Page No.</b>
Candidate's Declaration	i
Acknowledgement	ii
Abstract	iii
Contents	iv
List of Tables	vii
List of Figures	viii
<b>CHAPTER 1 INTRODUCTION</b>	<b>1</b>
1.1 GENERAL	1
1.2 NEED OF THE STUDY	2
1.3 ORGANIZATION OF THESIS	3
<b>CHAPTER 2 DEM ACCURACY AND ACQUISITION METHOD</b>	<b>4</b>
2.1 INTRODUCTION	4
2.2 ACCURACY ASSESSMENT OF DEM	4
2.3 EVALUATIONS OF DEM ACCURACY	5
2.3.1 Slope Aspect Accuracy	5
2.3.2 Slope Inclination Accuracy	5
2.3.3 Slope Stability Accuracy	7
2.3.4 Drainage Pattern Accuracy	9
2.4 DEM ACQUISITION METHODS	11
2.4.1 Ground Survey	12
2.4.2 Photogrammetric Source	13
2.4.3 Cartographic Sources	14
2.5 FACTORS EFFECTING DEM ACCURACY	16

2.6 APPLICATION OF DEM	17
2.6.1 Civil Engineering	17
2.6.2 Military Engineering	18
2.6.3 Hydrology	18
2.6.4 Geomorphology	18
2.6.5 Landscape Modeling	19
2.6.6 Mapping	20
2.7 DEM DERIVATIVES AND THEIR APPLICATION	21
<b>CHAPTER 3 BACKGROUND OF SATELLITE PHOTOGRAMMETRY</b>	<b>23</b>
3.1 GEOMETRY OF PHOTOGRAPHS	23
3.1.1 Collinearity Condition	23
3.1.2 Coplanarity Condition	24
3.1.3. Discussion of the two approaches	25
3.2 TRANSITION IN PHOTOGRAMMETRY	26
3.3 NEW DEVELOPMENT IN DIGITAL PHOTOGRAMMETRY	29
3.4 HARDWARE AND SOFTWARE CONFIGURATION	30
3.5 NEW DPW DESIGN	32
3.6 SATELLITE PHOTOGRAMMETRY AND SOFTWARE USED	37
3.7 DESCRIPTION OF RPC FILE	39
3.8 IKONOS RPC MODEL	40
<b>CHAPTER 4 DATA USED AND METHODOLOGY</b>	<b>42</b>
4.1 DATA USED	42
4.2 WORK FLOW DIAGRAM OF GENERATION OF DEM WITH RPC	43
4.3 GENERATING DEM USING GEOMATICA 10.0	44
4.4 GENERATING DEM USING ERDAR 8.6	48

4.5 GENERATING DEM USING ENVI 4.3 10.0	51
<b>CHAPTER 5 RESULTS AND CONCLUSIONS</b>	<b>54</b>
5.1 RESULTS AND ANALYSIS	
5.1.1 Analysis of DEM Generated by Different Softwares	54
5.1.2 Analysis of Tie Point Generated through Photogrammetric Software	55
5.1.3 Comparison of Elevation between Three Software	59
5.2 RESULT AND CONCLUSIONS	64
5.3 FURTHER STUDY RECOMMENDATIONS	65
<b>REFERENCES</b>	<b>66</b>

## LIST OF TABLES

---

<b>Table No.</b>	<b>Title</b>	<b>Page No.</b>
Table 2.1	Comparison of Various DEM Acquisition Methods	11
Table 2.2	Comparison of the Accuracy of DEM Data Obtained by Different Techniques	16
Table 2.3	DEM Derivatives and their Application	21
Table 2.3	DEM derivatives and their application	
Table 5.1	Statistics of DEM Source	55



## **LIST OF FIGURES**

<b>Figure No.</b>	<b>Title</b>	<b>Page No.</b>
Figure 2.1	Accuracy of Slope Aspect according to Spatial Resolution	6
Figure 2.2	Accuracy of Slope Aspect according to Spatial Resolution	6
Figure 2.3	Accuracy of Slope Inclination according to Spatial Resolution	7
Figure 2.4	Accuracy of Slope Inclination according to Spatial Resolution	7
Figure 2.5	Illustration of Fellenius Method	8
Figure 2.6	Accuracy of Safety Factor according to Spatial Resolution	8
Figure 2.7	Accuracy of Safety Factor according to Spatial Resolution	9
Figure 2.8	Accuracy of Drainage Pattern according to Spatial Resolution	10
Figure 2.9	Accuracy of Drainage Pattern according to Spatial Resolution	10
Figure 3.1	Collinearity and Coplanarity Condition	25
Figure 4.1	IKONOS Imagery of Study Area	42
Figure 4.2	Work Flow Diagram of Generation of DEM with RPC	43
Fig 5.1(a)	DEM using ERDAS	54
Fig 5.1(b)	DEM using ENVI	54
Fig 5.1(c)	DEM using PCI	54
Fig 5.2	All Tie Points	57
Fig 5.3	Erroneous tie points	57
Fig 5.4	Graph between Elevation and Number of Points	59
Fig 5.5(a)	Water Bodies in ERDAS Imagine	60

Fig 5.5(b)	Water Bodies in ENVI	60
Fig 5.5(c)	Water Bodies in PCI Geomatica	61
Fig 5.6	Contour Lines in ENVI	61
Fig 5.7	Contour Lines in PCI	61
Fig 5.8	Contour Lines in ERDAS	62
Fig 5.9	Contour Interval	62
Fig 5.10	Density slice of peak in ENVI	63
Fig 5.11	Density slice of next peak in ENVI	63

# CHAPTER 1

## INTRODUCTION

---

### 1.1 GENERAL

A Digital Elevation Model (DEM) is a digital representation of a portion of the earth's surface. In a DEM, earth's surface is represented as spatially referenced regular points where each grid point represents a ground elevation value. It has long been known that DEMs have a potential for solving theoretical and applied problems in earth science

DEMs represent elevation data and are the principal digital data source for slope and aspect map coverages used in geographic information system (GIS) analysis for resource management. Elevation data can be represented digitally in many ways including a gridded model (where elevation is estimated for each cell in a regular grid), a triangular irregular network, and contours.

There are two main approaches to generating a DEM:

- 1) Interpolating the regular grid from an irregularly distributed elevation data set
- 2) Generating the grid directly from remotely sensed imagery using photogrammetric techniques.

In this work I used photogrammetric approach to generate DEM because Photogrammetry provides the most frequently used data sources and techniques for generating DEM's, either by direct generation of DEM's or indirectly via its use in topographic mapping for production of contour lines. Photogrammetry either involves stereoscopic techniques for interpretation of aerial photography or digital image correlation applied to aerial photographs.

Advantage of using photogrammetric approach:

- Remote sensing avoids the need to gain overland access to the area being surveyed across potentially remote and hazardous terrain.
- Data with a wide aerial coverage can be acquired in a relatively short time.
- There is no need for accurate topographic maps to be available.

However, there are also a number of potential problems associated with obtaining aerial photography in mountainous areas, including:

- Frequent cloud cover and lengthy snow cover limiting the opportunities for good photography may reduce the aerial coverage.
- The military or political sensitivity of a number of mountain regions may restrict the availability of data, or reduce the opportunities for flying aerial photography;
- Dense tree cover can obscure the ground surface.

In many situations directly generating a DEM from aerial photography is not a practical option due to the costs of purchasing suitable photography, software and hardware, non-existence of suitable photography or lack of suitably experienced personnel.

## **1.2 NEED OF THE STUDY**

The new phase of transition is known as “softcopy” or digital Photogrammetry. By digital Photogrammetry, we mean input data are digital images or scanned photographs. DEM extraction is one of the most time-consuming aspects of the map production process. Automating this process can speed the overall map production

process by a significant factor. Fortunately, the number of procedures and algorithms has been proposed for automatic DEM generation in batch mode. Today, many photogrammetric and mapping companies use automatic DEM collection software. A regular DEM data of a stereo pair of frame photography can be created in less than two hours with the accuracy of 1/10000 of flying height. Characteristic features such as break lines, boundary areas, and abrupt changes still are digitized manually. In such cases the accuracy becomes most important factor to analysis the DEM for different application.

### **1.3 ORGANIZATION OF THESIS**

In this chapter has been discussed about the general concept of DEM and how photogrammetric approach is important in generation of DEM/DTM. Chapter 2 is continuing the discussion about the DEM including some accuracy aspects of DEM finally it ended with the application of DEM. Chapter 3 consist the discussion about the concept behind the satellite Photogrammetry. It also included the hardware and software used for generation of DEM and the role of digital Photogrammetry or satellite Photogrammetry. This chapter also provides the information about the RPC file that contains camera/sensor parameters. Chapter 4 is the methodology of work, how the thesis work is carried out, what were the steps, which data is used and different software used in this study. Chapter 5 is the results and conclusion of the study. Finally this work is ended with the references which help me to do this work.

### DEM ACCURACY AND ACQUISITION METHOD

---

#### 2.1 INTRODUCTION

Within the context of Geographical Information Systems (GIS), several types of surface models are being used in a spatial modeling environment. DEM is a fundamental requirement for many GIS applications, both directly due to the influence of elevation on many environmental phenomena and indirectly due to the influence of variables derived from a DEM such as gradient and aspect on environmental phenomena and processes. Till now DEM generating from Survey of India topomaps, ground survey and photogrammetric data sources. But user needs accuracy, which is important for various applications such as hydrology, geomorphology, ecology and other disciplines. Therefore it is Important to know the accuracy to be expected from different sources. This paper summarizes different DEM methods and the expected accuracy.

#### 2.2 ACCURACY ASSESSMENT OF DEM

Accuracy is most important factor that influencing the overall quality of a data set. According to Foote and Huebner (1997) describes how similar a data set is to the real world or true values. Error is a specific measurement of the different between a value in a data set and the corresponding true values. Goodchild et al (1994) define accuracy as the difference between values recorded in a spatial data set and modelled or assumed values. They define error as the difference between the data set values and the true values. When dealing with continuous phenomena and their representation in GIS as surfaces, it is impossible to measure all true values and hence calculate all errors. So the true values

must be modelled or estimated. So in the case of continuous phenomena one deals with accuracy indices derived from a limited number of error measurements.

There are two issues to consider when using sample points to check DEM accuracy. First, how should the sample points be selected? Second, how can measurements of a higher order of accuracy be obtained? Practically it will not be possible to measure true elevation from ground because of time and accessibility. Instead of determining the absolute accuracy of the DEM more commonly to measure the relative accuracy in comparison with sample point measurement known to be of a higher order of accuracy (Akira et al, 2003). These issues are examined below followed by a review of ways of measuring accuracy.

## **2.3 EVALUATIONS OF DEM ACCURACY**

### **2.3.1 Slope Aspect Accuracy**

A slope aspect can be expressed from DEM, which is one of the most important items for topographical analysis. In this study, the slope aspect means a direction along the maximum slope inclination at one target pixel. Figure 2.1 shows histogram of difference between original aspect data and resampled aspect data of each grid size. The histograms show symmetrical form. Figure 2.2 shows a relationship between grid size and percentage of correct pixels. The correct percentage in every resampling method has tendency to drop with grid size increase. Maximum value sampling showed the highest accuracy, minimum value sampling showed the worst accuracy.

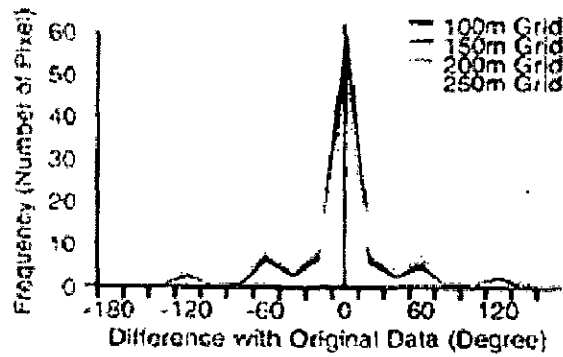


Figure 2.1 Accuracy of Slope Aspect according to Spatial Resolution

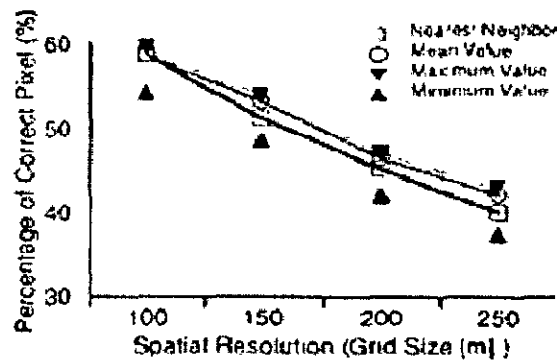


Figure 2.2 Accuracy of Slope Aspect according to Spatial Resolution

### 2.3.2 Slope Inclination Accuracy

A slope inclination can be expressed from DEM, which is also one of the most important items for topographical analysis. In this study, the inclination means maximum slope inclination at one target pixel. Figure 2.3 shows histogram of difference between original inclination data and resampled inclination data of each grid size. The histograms show asymmetrical form that is shifted to right. It means the resampled inclination data became gentle slope. Because, detailed terrain is gnarred by grid size increase. Figure 4 shows a relationship between grid size and percentages of correct pixels. In case of slope in clinat in, correct pixel means difference with original data indicates inside of 20



degree. The nearest neighbor sampling almost showed the highest accuracy, mean value sampling showed the worst accuracy.

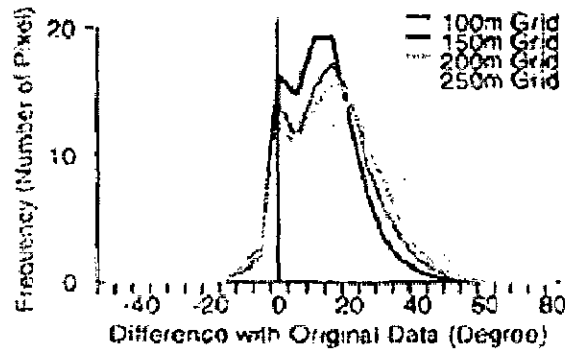


Figure 2.3 Accuracy of Slope Inclination according to Spatial Resolution

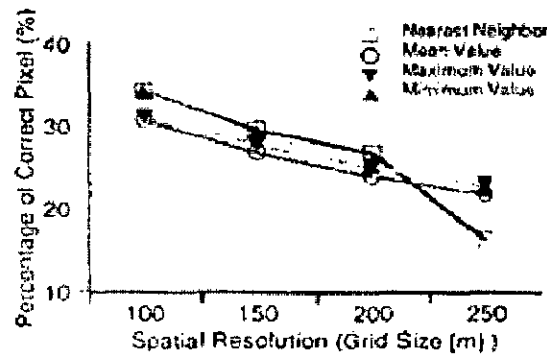


Figure 2.4 Accuracy of Slope Inclination according to Spatial Resolution

### 2.3.3 Slope Stability Accuracy

A slope stability analysis is popular application of DEM. Sometime we generate land slide risk map or slope failure risk map from DEM. The slope stability which means safety factor was calculated by a ratio between driving moment and resistance moment along the target profile. When the safety factor is calculated on every pixel, such risk map can be generated. Fellenius method as slope stability analysis was selected in this study. In this method, landslide type is assumed rotational slip (Figure 2.4). A landslide soil is divided into some slices in order to calculate moment along the critical circle (Fig 2.5).

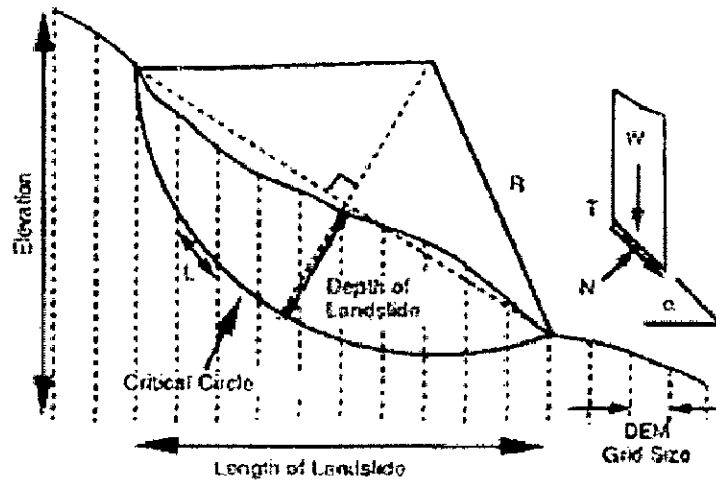


Figure 2.5 Illustration of Fellenius Method

Figure 2.6 shows histogram of difference between original slope stability data and resampled slope stability data of each grid size. The histograms show asymmetrical from that is shifted to left. It means the resampled safety factor. This situation will make serious problem because of under estimation. Figure 2.7 shows a relationship between grid size and percentages of correct pixels. In case of slope stability, correct pixel means difference with original data indicates inside of 0.2 ( $F_s$ ). The nearest accuracy. However, each trend was very similar.

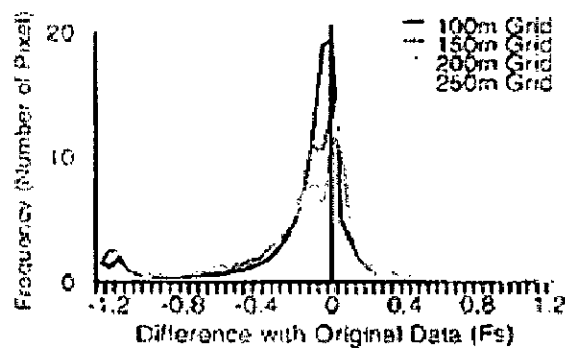


Figure 2.6 Accuracy of Safety Factor according to Spatial Resolution

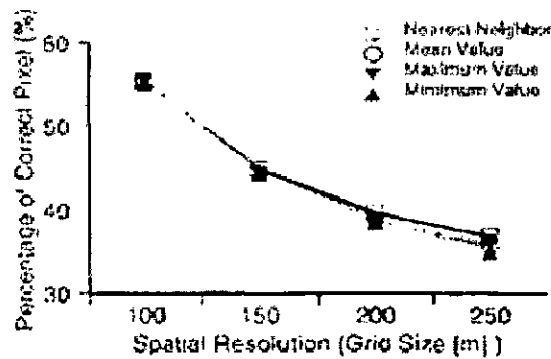


Figure 2.7 Accuracy of Safety Factor according to Spatial Resolution

### 2.3.4 Drainage Pattern Accuracy

A runoff analysis or a drainage pattern generation is very popular application of DEM. Usually, such analysis can be carried out by using a grid series tank model. A precipitation is supplied to each DEM grid that is one of the tanks. The inlet content must discharge to next grid according to slope aspect and velocity. That is to say flow tracking. The slope aspect can be calculated from DEM, the velocity can be estimated from slope inclination which is also calculated from DEM. And the flow in the grid can be expressed by a continuous equation as follows;

$$Q_{t+\Delta t} = (\Delta q_{in} - \Delta q_{out}) \Delta t$$

**Q:** Remaining Content (m<sup>3</sup>)

**q<sub>in</sub>:** Inlet (m<sup>3</sup>/s)

**q<sub>out</sub>:** Outlet (m<sup>3</sup>/s)

**Δt:** Time (s)

By using previous equations, drainage pattern can be drawn. In this study, a parameter of infiltration was given, 1.0, because purpose is just DEM evaluation. Figure 2.8 shows histogram of difference between original runoff data and resampled runoff data as each grid size. The histograms show symmetrical form. Figure 2.9 shows a relationship between grid size and percentages of correct pixels. In case of runoff analysis, correct pixel means difference with original data is inside of 20m<sup>3</sup>/s. The nearest neighbor sampling showed the highest accuracy, minimum value sampling showed the worst accuracy. The accuracy of runoff analysis indicates higher than slope stability analysis.

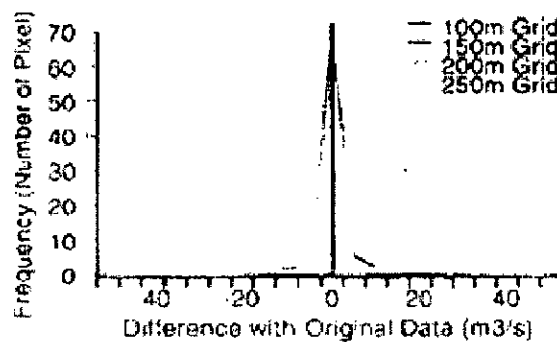


Figure 2.8 Accuracy of Drainage Pattern according to Spatial Resolution

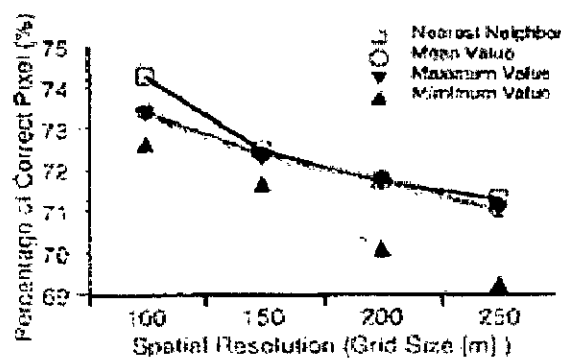


Figure 2.9 Accuracy of Drainage Pattern according to Spatial Resolution

## 2.4 DEM ACQUISITION METHODS

For DEM acquisition method

- 1) We have to select the sample control points from a more accurate data source, and presuming that this sample is sufficiently large and representatively distributed, the difference between the DEM and control point's elevation values can be calculated.
- 2) The next consideration is how to turn this set of individual elevation errors into an estimate of the DEM's accuracy.

The sources of digital elevation data under the three main headings of ground survey sources, photogrammetric sources and cartographic sources. LIDAR data are of high quality and great uses in the future either to create DEMs and DSM or, more probably, to check the quality of DEM, other sources and their accuracy mentioned in table 2.1.

Table : 2.1 Comparison of Various DEM Acquisition Methods

<b>Acquisition Methods</b>	<b>Accuracy of Data</b>	<b>Speed</b>	<b>Cost</b>	<b>Applications Domain</b>
Traditional Surveying	High (cm-m)	Very Slow	Very high	Small areas
GPS survey	Relatively high (cm-m)	Slow	Relatively high	Small areas
Photogrammetry	Medium to high (cm-m)	Fast	Relatively slow	Medium to large areas

Space Photogrammetry	Low to medium (m)	Very fast	Low	Large areas
InSAR	Low (m)	Very fast	Low	Large areas
Radargrmmetry	Very low (10m)	Very fast	Low	Large areas
LIDAR	High (cm)	Fast	High	Medium to large areas
Map digitization	Relatively low (m)	Slow	High	Any area size
Map scanning	Relatively low (m)	Fast	Low	Any area size

(Source: Zhilin Li et al 2005)

#### 2.4.1 Ground Survey

Ground survey is the basic and first technique to generate DEM . Ground survey sources of elevation data involve actual measurement of elevation in the field. For that purpose instrument is used total station ,GPS to collect the the data .

Total stations can be used to create a network of surveyed points covering an area. The equipment allows highly accurate planimetric and altitudinal measurements. The data quality is also enhanced by the use of the surveyor's local knowledge to adapt the survey to incorporate key features and significant sample points, which provide a good representation of the terrain.

GPS equipment has been considered as potentially more practical for ground survey in mountain environments (Heywood et al., 1999). Equipment can be cheaper and more portable than traditional surveying hardware and data collection can be faster. However, a number of limitations do not currently make GPS a viable alternative for collecting a complete data set for creating a DEM. These limitations include inaccessibility, the trade off between portability and accuracy and between speed and accuracy, the high potential for poor satellite visibility and the difficulties of differential correction in mountainous regions.

#### **2.4.2 Photogrammetric Source**

As mention in introduction part Aerial photography and satellite imagery can be used to derive digital elevation data. At present, the resolution of suitable imagery and the sophistication of processing mean that elevation data derived from satellite imagery is usually only suited to small scale applications covering large areas, such as national, continental or global studies (Lillesand & Kiefer, 2000). The properties of the imagery those influences the accuracy of data captures are: scale and resolution of the aerial photography; the flying height at which the photography was obtained; and, the base to height ratio, or geometry, of the overlapping photographs. These properties are inter-related and it is their combined nature, which determines the accuracy of the stereoscopic techniques. Both the minimum vertical interval of the contours that can be derived and the scale of the DEM that can be produced are also dependant on these image characteristics. A compromise must be made between the geometry and scale, or resolution, of the photography.

### 2.4.3 Cartographic Sources

As (Ravibabu and Jain Kamal, 2005) Most DEMs with grid spacing of 50m or less are produced from cartographic data sources. Contour lines and spot heights on most topographic maps have originally been derived using the stereoscopic techniques. Accuracy is influenced by equipment, map distortion and operator or machine error. The accuracy of the equipment, in terms of the coordinates recorded, will be slightly less than the resolution, or precision, of the equipment. This precision will be in the range of 50 $\mu$ m to 100 $\mu$ m. At a map scale of 1:10,000 this equates to 0.5m to 1m. Over a large format paper-based map sheet distortion, in the form of stretch or shrinkage, of several millimetres can occur. At the 1: 10,000 scale this equates to an on-the-ground error of 10m or more. Regular scale changes can be removed to reduce the severity of distortions by recording the apparent location of control points on the map and then performing affine transformations on the digitised data. Operator and machine error is of more significance. On-line display of the digitised data and interactive editing reduce the likelihood and extent of such error. However, the potential for undetected errors remains important. Additionally, the extent of these errors is hard to quantify as it is determined by the skill and patience of the individual operator.

Taking into consideration all the above error sources, Li (2005) states that the horizontal accuracy of digitised contours will lie in the range of 0.1mm to 0.25mm RMSE (Ravibabu and Jain Kamal, 2005). This equates to 1m to 2.5 m on the ground at 1:10,000 scale. When obtaining digital elevation data from cartographic contour lines, a vertical error can only be caused by the operator tagging the wrong elevation value to a



contour line. However, although displacement of a contour is horizontal, this will cause an apparent vertical error by the time a continuous DEM surface is.

More meaningful information on the overall spread of error values is provided by the root mean squared error (RMSE), standard deviation of error and percentiles (Aurora et al 2005). The RMSE is easy to calculate, report and understand – it is just a single number. However, RMSE only gives a good description of error spread when the mean error is zero (Monckton, 1994; Wood, 1996).

**Equation :** Root Mean Squared Error (RMSE)

$$RMSE = \sqrt{\frac{\sum_i^n (Z_i - Z_j)^2}{n}}$$

Where  $z_i$  and  $z_j$  are two corresponding elevation values (e.g. DEM cell value and corresponding sample point elevation) and  $n$  is the number of sample points.

Wood (1996) identifies a second problem with use of RMSE. Relative relief and scale of measurement influence the magnitude of the RMSE value, so comparison between areas is difficult. He proposes using an accuracy ratio (RMSE divided by a measure of relative relief; Equation ) to remove the effects of relative relief.

**Equation :** Accuracy Ratio (a)

$$a = \sqrt{\frac{\sum_i^n (Z_i - Z_j)^2}{\sum_i^n (Z_i - \bar{Z}_j)^2}}$$

Where  $z_i$ ,  $z_j$  and  $n$  are as in Equation 4 and  $\bar{Z}_j$  is the average DEM elevation.

## 2.5 FACTORS EFFECTING DEM ACCURACY

The accuracy of DEM is a function of a number of variables such as the roughness of the terrain surface, the interpolation function, interpolation methods and other three attributes (accuracy, density, and distribution) of the source data (Li 1990, 1992)

Mathematically,

$$\mathbf{ADEM = f (CDEM, Mmodelling, R Terrain, A Data, D Data, DN Data, 0)}$$

Where A DEM is the accuracy of the DEM, CDEM refers to the characteristic of the DEM surfaces, Modeling is the method used for modeling DEM surface, R Terrain is the roughness of the terrain surface itself, A Data is Accuracy, D Data is distribution, DN Data is density of the DEM source data and 0 is denotes other element (Li 2005). The accuracy of contour can be written as:  $mc = mh + mp \times \tan \alpha$

Table 2.2 : Comparison of the Accuracy of DEM Data Obtained by Different Techniques

Methods of data acquisition	Accuracy of Data
Ground measurement (including GPS)	1-10cm
Digitized contour data	About 1/3 of contouring interval
Laser altimetry	0.5-2m
Radargrammetry	10-100m
Aerial Photogrammetry	0.1-1m
SAR interferometry	5-20m

(Source: Zhilin Li, et al 2005)

Where  $m_h$  refers to the accuracy of height measurement,  $m_p$  is the planimetric accuracy of the contour line,  $\alpha$  is the slope angle of the terrain surface and  $m_c$  is the overall height accuracy of the contour, including the effects of planimetric errors. The overall accuracy if digitized contour data will be within a 1/3 contouring interval. The accuracy of DEM source data from various sources is summarized in Table 2.2.

## **2.6 APPLICATION OF DEM**

Digital Elevation Models (DEM) are playing an increasingly important role in many technical fields of Geographical Information Systems (GIS) development, including earth and environmental sciences, hazard reduction, civil engineering, landscape planning, hydrology and commercial display. 3-dimensional information of the topography of the earth surface help us in understanding our vulnerable environment and secure a more sustainable management and use of our environmental resources. The improvement of sensor and satellite imaging technologies enabled the researchers to generate DEM using remotely sensed data. These data can be started to use as not only the two-dimensional (2-D) but also three-dimensional (3-D) information sources with usage of the DEM: Present paper summarized DEM importance in various applications.

### **2.6.1 Civil Engineering**

The first application of DEM is in civil engineering, more precisely, highway engineering. In 1957, Roberts proposed the use of DEMs for highway design after that Miller and Laflamme in 1958 used the data to set up a cross-section (profile) model and coined the concept of DEMs for the first time. The development of a transportation network is complicated, aiming to provide a network to satisfy the needs of society

### **2.6.2 Military Engineering**

Flight Simulation: in simulation, the DEM plays an important role. 3D rendering techniques are employed to simulate the terrain. Texture and other attributes can also be mapped onto the DEM surface to generate realistic scenery. To simulate scene changes while flying, the “flythrough” techniques is used. DEMs can also be used to guide cruise missiles. This is done by matching the DEM surface stored in the computer with the real world sensed by the detectors on board the cruise missile.

### **2.6.3 Hydrology**

Demands for hydrologic prediction tools that are better able to utilize information about spatial variations in precipitation, as well as land surface characteristics such as vegetation, soils, and topography, are driving the evolution of spatially distributed hydrologic models. Digital elevation models (DEMs), which are used to represent topographic controls on incoming shortwave radiation, precipitation, air temperature, and downslope moisture movement, form the foundation for such models (Storck et al., 1998). Previous studies have found that spatially distributed hydrological models are sensitive to DEM horizontal resolution, due especially to its influence on computed slopes and related model-derived quantities such as surface saturation extent (Zhang and Montgomery, 1994; Wolock and Price, 1994)

### **2.6.4 Geomorphology**

Digital elevation data has tremendous, but often under-utilized, potential to create highly useful GIS digital data layers for many natural resource applications. Automated interpretation of digital elevation data has, until recently, often been limited to the calculation of a basic set of terrain derivatives supported by most commercial GIS

software, namely slope gradient, aspect, profile and plan curvature. Customized extensions to GIS software often allow additional indices to be computed including hill shade illumination or solar radiation input, pathways for idealized overland flow, delineation of watershed or catchments boundaries and definition of inter-visibility between land surface elements. Numerous researchers have suggested ways in which indices computed from digital elevation data might help define landform-based units to act as relatively permanent spatial and structural entities for soil, terrain or ecological maps. However, no commercially available GIS systems have integrated these individual capabilities with an easy-touse capability for automatically computing landform-based spatial entities (e.g. landform facets or landform types). Research has shown that it is possible to predict a wide variety of sub-surface and soil attributes based on analysis and classification of variation in the terrain surface from a high resolution digital elevation model (DEM).

### **2.6.5 Landscape Modeling**

The potential of digital elevation models for studying and understanding landscape relationships is being realized. Digital elevation models are digital representations of the land surface (Burrough 1986). They may be either in vector or raster format, with the latter being most common because map calculations and topographic attributes are more easily calculated. Elevation data for DEM generation may be obtained through primary or secondary methods. Primary DEMs are produced from elevations measured directly in the field, and are often more accurate than their secondary counterparts (Chang and Tsai 1991). The accuracy of primary DEMs is in part dependent upon whether the data points selected represent significant landscape features, such as

slope breaks and ridgelines (Carter 1988). Secondary DEMs are derived from digitizing topographic contours and subsequently, interpolating elevation values (Chang and Tsai 1991). The interpolation process, though, often results in DEMs with elevations biased towards that of the contours (Moore et al. 1993b).

## **2.6.6 MAPPING**

To make images useful as backdrops for other thematic information and base maps, it is desirable that the images have characteristics similar to those of maps. This means that the same scaling, orientation and projection into a geo-referencing system should be adopted. To accomplish this, a number of requirements must be fulfilled. Generation of orthoimages from remote sensing images is in fact a process of coordinate transformation and geometric correction (Baltsavias et al 1996, and O. Hofmann et al 1984). It has been well known that terrain and imagery method have great impacts on coordinate and geometric distortions of the obtained images. Conventional orthorectification of large-scale aerial images only considers geometric distortions caused by photogrammetry and terrains. Thus digital terrain model (DTM) representing not only coordinates of image area but also the altitude of the region's terrain is the prerequisite for the orthorectification (F. Amhar et al 1998 and W. Schickler et al 1998). Generation of digital orthophotos from SPOT images has been examined (Chen 1993). Zheng et al. (1997) orthorectified space shuttle photographs in coastal area and Zhou et al. presented orthorectification of satellite photographs for Greenland. Since SPOT and other satellite images represent imagery at high altitude, terrain impacts on geometric distortions are relatively small. These characteristics of high altitude imagery systems make orthorectification for true orthoimage relatively easy. However, when imagery is at low

altitude for large-scale images in urban areas, difficulties in true orthoimage generation are much more than that for high altitude imagery system because serious occlusions and poor visibility as result of urban buildings. Though several studies have been reported, efforts still required improving the state-of-art. In the study we intend to develop a methodology based on digital surface model (DSM) for true orthoimage generation from large-scale aerial images with high buildings.

### 2.7 DEM derivatives and their application

Elevation is just one of a number of properties of the terrain of an area which influence the distribution of environmental phenomena and the nature of environmental processes. The most important of these terrain properties can be grouped as attributes of surface form or surface topology and various environmental indices, which can be calculated by combining surface form and surface topology measures. DEM are widely used in many applications such as hydrology, geomorphology, ecology and Table shows other applications.

Table 2.3 DEM Derivatives and Their Application

Derivative	Description	Applications
Elevation	---	Potential energy determination; climate variables; cut and fill calculations.
Gradient	Rate of change of elevation	Overland and sub-surface flow; land capability assessment; vegetation types;
Aspect	Compass direction of steepest downhill gradient	Solar irradiance; evapotranspiration; vegetation types.
Profile	Rate of change of gradient	Flow acceleration; erosion/deposition

curvature		zones; soil and land evaluation indices.
Plan curvature	Rate of change of aspect	Converging/diverging flow; soil water properties.
Flow direction	Direction of downhill flow	Computing surface topology; material transport.
Upstream area	Number of cells upstream of a given cell	Watershed delineation; volume of material passing through a cell.
Stream length	Length of longest uphill path upstream of a given cell	Flow acceleration; erosion rates; sediment yield.
Stream channel	Cells with upstream area greater than a specified threshold	Location of flow; flow intensity; erosion/sedimentation.
Ridge	Cells with no upstream area	Drainage divides; vegetation studies; soil, erosion and geological analysis.
Wetness index	$\ln(\text{upstream area}/\tan(\text{gradient}))$	Index of soil saturation potential.
Stream power index	Upstream area * $\tan(\text{gradient})$	Index of the erosive power of overland flow
Viewshed	Zones of intervisibility	Visual impact studies.
Irradiance	Amount of solar energy received	Vegetation and soil studies; glaciology.

(Source: Burrough & McDonnell, 1998)



## BACKGROUND OF SATELLITE PHOTOGRAMMETRY

---

### 3.1 GEOMETRY OF PHOTOGRAPHS

A photograph is a projective transformation from 3-D object space to 2-D image plane through perspective projection. In Photogrammetry, a data reduction approach basically involves in recreation of the 3-D geometry of object space responsible for image formation, in one or other way. The basic equations governing the formation of image and its recreation are the equation of collinearity and coplanarity. These equations are fundamental equations of Photogrammetry and provide basis for metric determination from photographs. These are discussed here in brief.

#### 3.1.1 Collinearity Condition

Collinearity is the condition that exposure station, any object point, and its photo image all lie along a straight line (Wolf,1988). The condition is illustrated in Figure, where L, a, and A lie along a straight line. Two equations express the collinearity condition for any point on a photo.

#### Collinearity Equations

$$\begin{aligned}
 x - x_0 &= -f \left[ \frac{m_{11}(X - X_L) + m_{12}(Y - Y_L) + m_{13}(Z - Z_L)}{m_{31}(X - X_L) + m_{32}(Y - Y_L) + m_{33}(Z - Z_L)} \right] \\
 y - y_0 &= -f \left[ \frac{m_{21}(X - X_L) + m_{22}(Y - Y_L) + m_{23}(Z - Z_L)}{m_{31}(X - X_L) + m_{32}(Y - Y_L) + m_{33}(Z - Z_L)} \right] \\
 X - X_L &= (Z - Z_L) \left[ \frac{m_{11}(x - x_0) + m_{21}(y - y_0) + m_{31}(-f)}{m_{13}(x - x_0) + m_{23}(y - y_0) + m_{33}(-f)} \right] \\
 Y - Y_L &= (Z - Z_L) \left[ \frac{m_{12}(x - x_0) + m_{22}(y - y_0) + m_{32}(-f)}{m_{13}(x - x_0) + m_{23}(y - y_0) + m_{33}(-f)} \right]
 \end{aligned}$$

Where

$x$  and  $y$  are the photo coordinates of an image point,

$X, Y, Z$  are the ground coordinates of the object point,

$X_L, Y_L$  and  $Z_L$  are the ground coordinates of the exposure station,

$f$  is the camera focal length,

$m$ 's are the rotation angles  $\omega, \phi$  and  $\kappa$ , which the camera axis makes

with the plumb direction.

### 3.1.2 Coplanarity Condition

Coplanarity is the condition that the two exposure station of a stereopair, any object and its corresponding image points on the two photos all lie in a common plane. The basic idea of the coplanarity approach is to formulate a constraint such that the projection planes in image space and object space become identical (coplanar). Such a constraint can be formulated as

$$\lambda \mathbf{R} \mathbf{n}' = \mathbf{n}$$

with  $\lambda$  a scale factor,  $\mathbf{R}$  the attitude matrix,  $\mathbf{n}'$  the normal of the plane defined by the perspective center  $C$  and image line  $L'$ , and  $\mathbf{n}$  the normal of the plane defined by the perspective center  $C$  and control line  $L$ .

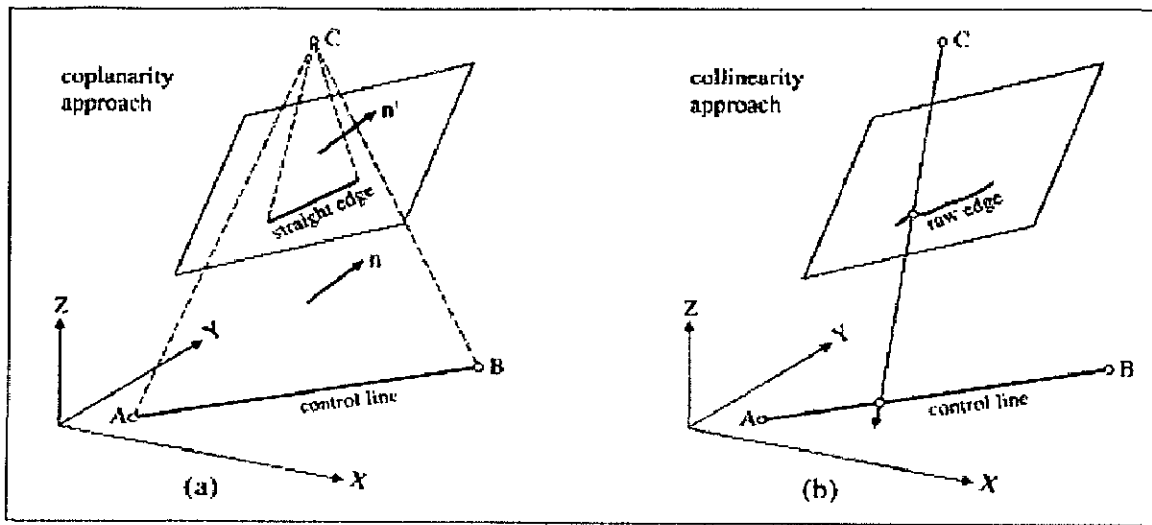


Fig 3.1 Collinearity and Coplanarity Condition

### 3.1.3. Discussion of the two approaches

The coplanarity approach is intuitively simple. Nevertheless, it has several disadvantages. For one, it restricts the shape of features to straight lines. In contrast, the collinearity model can easily be extended to higher-order features, for example, conic sections, polynomials, or any 3D curve that allows a parametric representation.

Another major difference between the two methods lies in the representation of the feature in image space. The coplanarity model requires a straight image line while the collinearity model works with any point of the image line, for example, edge pixels. Usually, it is not possible to determine straight lines in images directly. Rather, straight lines are obtained by a sequence of processes, such as detecting, linking, and segmenting edges. The collinearity model can work with lower level primitives (e.g., edge pixels), which may be advantageous at times. On the other hand, it also copes with straight lines by taking their end points. Using all pixels of the image line or only the two endpoints of the fitted line lead to identical results if the covariance matrix of the line fitting process is used

as the weight for the two end points. In this way, the collinearity model can be seen as combining the line fitting process with the subsequent orientation and/or reconstruction task.

### **3.2 TRANSITION IN PHOTOGRAMMETRY**

In general, the invention of photography, airplane, and computer brought about the following phases in Photogrammetry (Konecny, 1985):

1. Stereo Photogrammetry and analog stereo plotter
2. Analytical Photogrammetry
3. Computer-assisted Photogrammetry
4. Digital Photogrammetry

The first stage of development, known as analog Photogrammetry, lasted about 30 years. Aerial survey techniques became a standard procedure in mapping. There was no automation involved in any modern sense. Measurement and drafting were done manually. Classical analog stereo plotters are gradually disappearing from the market and are not being manufactured anymore, although quite a large number of them are still in practical use.

The second phase of development, known as analytical Photogrammetry, began in the 1950's due to the advent of computers. Many analytical techniques were developed and computer-aided- Photogrammetry and mapping were designed. The first operational photo triangulation program became available in the late sixties (Ackermann, Brown, Schut, to name a few). Another area of development in this period was the generation of DEM and manual feature extraction. These were also the result of consistent application of computer methods. In these applications, the operator handles the task of

measurement with very few computer-assisted operations. It is the data processing that has made photo triangulation, DEM generation, and feature extraction very efficient and reliable techniques.

Perhaps the most important development in this period was the invention of the analytical stereo plotter by Helava (1957). The analytical stereo plotter is essentially an instrument with a built-in digital computer as its main component, which handles the physical and mathematical relationship between object (ground) space and image space. The analytical plotters were introduced into the market during the 1976 International Society of Photogrammetry and Remote Sensing (ISPRS) Congress. Intergraph's InterMap Analytic (IMA), a flexible photogrammetric workstation that combines interactive graphics and an advanced stereo plotter, was introduced in 1986 (Madani, 1986).

The third phase of development, known as computer-assisted Photogrammetry, began in the early seventies when electronic plotting tables became available. Computer-assisted Photogrammetry has undergone great development by making use of computer technology and graphical data processing.

The early systems were mainframe based and designed by in-house expertise. Digital mapping systems were created on mini computers and were characterized by unstructured formats and internal proprietary formats. The next stage brought computer assisted design (CAD), workstation based systems. These systems had graphic displays that provided on-line graphics for reviewing and editing digitized data. Translators to the most common formats were typical, and database technology began to emerge in digital mapping systems. Interactive graphical workstations were the result of advances in this

period. Interactive graphic techniques changed the process of map compilation drastically in terms of flexibility and efficiency in the final output products.

The new phase of transition is known as “softcopy” or digital Photogrammetry. By digital Photogrammetry, we mean input data are digital images or scanned photographs. Digital Photogrammetry has its root in the late sixties when Hobrough (1968) began experimenting with correlation, even though the solutions were analog in nature. For almost 20 years, correlation techniques remained the only noticeable activity in digital Photogrammetry. Research efforts in digital Photogrammetry have increased tremendously in recent years due to the availability of digital cameras, satellite imagery, high quality scanners, increased computing power, and image processing tools (Sarajkoski, 1981). A digital photogrammetric system should perform not only all the functionalities that as analytical stereo plotter does, but should also automate some processes that are usually performed by operators (Madani, 1991). Two digital photogrammetric workstations were introduced during the XVI ISPRS Congress in Kyoto, 1988.

Since digital Photogrammetry is rather new, it is easy to generate a list of problems. In some aspects, the present state can be compared with analog instruments in the thirties or with analytical stereo plotters in the seventies. Most problems arise due to the extremely large size of digital images. An aerial photograph of 23 x 23 centimeters, scanned at 20 micrometers resolution, requires over 200 megabytes of storage. Storage of such a large amount of data is no longer a problem. Hard disks with gigabytes of storage capacity are available in most workstations and personal computers. Fast access and processing of such data is another problem. As an example, local transfer time of a

15-micrometers digitized aerial photo is a few minutes. Transmitting time of this image, through a telephone line, may be a few hours or even days. Creation of multi-resolution of digital images through image pyramids and compression/decompression techniques are some possible solutions to this problem.

### **3.3 NEW DEVELOPMENT IN DIGITAL PHOTOGRAMMETRY**

There are a number of important factors that caused this rather rapid development in Digital Photogrammetry (Dowman, 1991). Some of these factors may be summarized as:

- Availability of ever increasing quantities of digital images from satellite sensors, CCD cameras, and scanners.
- Availability of fast and powerful workstations/computers with many innovative and reliable high-tech peripherals, such as storage devices, true color monitors, fast data transfer, and compression/decompression techniques.
- Integration of all types of data in a unified and comprehensive information system such as GIS.
- Real-time applications such a quality control and robotics.
- Computer-aided design (CAD) and industrial applications.
- Lack of trained and experienced photogrammetric operators and high cost of photogrammetric instruments.

Because of these key technological advances; cost; labor; and new areas of applications (GIS and CAD), digital photogrammetric systems have been and are being designed. The main idea is to use digital images, scan the model area with a three-dimensional “floating mark” with sub-pixel accuracy. Then use a digital workstation to compile the required

features to form an intelligent description for an information system such as GIS and CAD systems.

The following sections provide some broad information about hardware and software configurations of a high-end digital photogrammetric workstation.

### **3.4 HARDWARE AND SOFTWARE CONFIGURATION**

An integrated digital Photogrammetry system is defined as hardware/software configuration that produces photogrammetric products from digital imagery using manual and automatic techniques. The output for such systems may include three-dimensional object point coordinates, restructured surfaces, extracted features, and orthophotos.

There are two major differences between a digital Photogrammetry workstation (DPW) and an analytical stereo plotter. The first and perhaps the most significant is input data. Most problems arise due to the extremely large size of the digital images. This alone can almost cause the photogrammetric workflow to grind to a halt if the image file is not handled properly. The most efficient way to handle large image files is through smart file formats and image compression techniques.

The second change brought on by the digital Photogrammetry system is a potential for automatic measurement and image matching that simply did not exist in the analytical stereo plotter environment. The automatic measurement and image matching techniques are the great value-added components that the new digital technologies bring to Photogrammetry (Madani, 1996).

The advent of low cost symmetric multiprocessing computers and very high performance frame buffers allowed us to consider a new solution to the DPW design.



The new DPW must satisfy both commercial and government Photogrammetry requirements. Furthermore, it should keep pace with the rate at which computer technology is changing.

A DPW system consists of the following components (Madani, 1991):

- Stereo Workstation
- Stereo viewing Device
- Command Selection and XYZ Movement Controller Devices

There are several types of stereo workstations, most of them commercially available, based on different data processing speed, data transfer rates, disk drive storage, graphics and color display capabilities, and other auxiliary devices.

In general, a digital Photogrammetry workstation can display imagery in a static (fixed) mode with a moving cursor or in a dynamic (roam) mode with a fixed cursor. In the static mode, the images stay fixed and the cursors move "over" them. The moving cursor mode does not require a very powerful image processing computing power. The images need to be processed only once for an entire window measurement. In the dynamic mode, the cursor is permanently positioned in the center of the display, with the images moving "behind" the cursors. This results in an operation, which is very similar to the analytical stereo plotter. The fixed cursor mode places high demands on the image processor, particularly because fractional pixel pointing is required. The display systems of these workstations are capable of switching from a 60-hz planar mode to a 120-hz non-destructive stereo mode.

The stereo effect may be achieved by an interface to the workstation's monitor by a special viewing device. There are a great variety of stereo technologies to choose from.

One of the very popular stereo technologies is to use a passive polarization system. This system consists of a binocular eyepiece and an infrared emitter. The eyepiece has liquid crystal (LC) shutters. A sensor on the eyepiece detects the infrared signals broadcasted by the emitter to switch the LC shutters in exact synchronization with the image fields as the monitor displays them. The active eyepiece is shuttered at 1/120 second providing stereo by allowing the left eye to view the left image while the right eye is blocked and the right eye to view the right image while the left eye is blocked. Thus each eye only sees its appropriate image.

### **3.5 NEW DPW DESIGN**

Next generation of DPWs must fulfill a basic set of requirements. Some of the main elements of the first generation DPWs were:

- Management of very large images
- Support for very large monitors
- Smooth and continuous roam across the entire image
- Stereo display in a window
- Stereo vector superimposition
- Fully functional data capture during roam

In addition to these fundamental requirements, a number of additional requirements had to be met to satisfy the needs of government organizations. These additional requirements were:

- 16 bit per pixel panchromatic stereo processing
- Bicubic interpolation
- 5x5 convolution filtering

- Automatic convolution filter selection during zoom
- Automatic dynamic range adjustment
- N bit to 8 bit display mapping and gamma correction
- On-the-fly eppipolar resampling

On-the-fly eppipolar resampling would enable production shops to eliminate the time-consuming batch resampling of images prior to stereo exploitation. The remaining requirements would greatly enhance the quality of the displayed imagery and relieve the operator from the very tedious tasks of image enhancement during exploitation.

In-line software JPEG image compression and decompression eliminates the need to have the uncompressed images anywhere on the system. Software JPEG compression and decompression allows the system to uncompress the images on the machine only at display time, and only that portion of the image to be displayed. This capability enables operators to store, backup, and transfer over the network images that are approximately 1/3 the size for black and white images or 1/10 the size for color.

In addition, other design goals are necessary to ensure that DPWs can keep pace with the rate at which technology is changing. Among these design goals are:

- Independence from custom hardware
- A single scalable executable
- Hosting on a platform with a large installed software base
- Hosting on a platform with a very high probability of maintaining backward binary compatibility

A careful review of these design goals led us to a symmetric multiprocessing (SMP) architecture. An examination of the workstation market for the late 1990s clearly

indicated that the only "open" system supporting SMP that was suitable for technical processing was Windows NT. In addition, the Open Graphics Library (OpenGL) had been ported to the operating system. Thus, the architectural launch pad became:

- Windows NT
- SMP aware software
- Open Graphics Library (OpenGL) for raster and vector operations

Digital Photogrammetry software configuration varies from one vendor to another. These systems provide the following capabilities:

- Enhance images for brightness and contrast
- Rotate, flip, and transpose imagery
- Display overview, full resolution, and detail imagery
- Measure fiducials, reseaux, pass points, and control points; manually, semi-automatically, or automatically
- Interior, relative, absolute, and bundle orientation
- Create eppipolar stereo models (if necessary) and image pyramids
- Display a digital stereo model for on-Compilation, DEM generation, and three-dimensional feature extraction
- Automatic aerial triangulation, DEM collection and linear feature extraction
- Manual collection of breaklines and other map features
- Graphic updates, while reviewing, roaming, and editing
- Stereo superimposed points, lines, and other map features while roaming
- Several editing options for a quick model set-up

Once interior orientation is performed on an image, its parameters are included in the definition of the pixel's coordinates. This relieves the operator from re-establishing the interior orientation in the case of re-measurement of previously used imagery. Image refinement, such as lens distortion, atmospheric refraction, and other systematic errors may be applied directly to the resample images. This reduction process leads to a great simplification of the real-time equations.

Automatic measurement of image coordinates of conjugate points for the computation of object coordinates is another task of the digital Photogrammetry. This task is referred to as "image matching". Since no unified or well understood theory of human vision exists up to now, a large number of algorithms for image matching have been proposed over the years (Ackermann, 1983, Gruen, 1985, Schenk, 1991, to name a few). The image matching can be accomplished by gray-level correlation, feature-based matching, or a combination of both. As long as good approximations (about few pixels) are available and the gray levels yield enough signals within the correlation windows, traditional correlation methods work well.

Resampling is involved in all geometric manipulations of images, such as rectification, rotation, zooming, and even positioning for sub pixel measurements. Digital imagery can be rectified and resample to normalize images on the fly by using interior and exterior orientation parameters. The generally titled images are projected onto a theoretical plane that is parallel to the model base, facilitating considerably the extraction of operator-specific image information and the matching of features. Different mathematical models, such as nearest-neighbor, bilinear, and cubic convolution are used

for resampling. The cubic convolution process provides the best image clarity. Nearest-neighbor and bilinear interpolation can be performed when a quick solution is desired.

DEM extraction is one of the most time-consuming aspects of the map production process. Automating this process can speed the overall map production process by a significant factor. Fortunately, the number of procedures and algorithms has been proposed for automatic DEM generation in batch mode. Today, many photogrammetric and mapping companies use automatic DEM collection software. A regular DEM data of a stereo pair of frame photography can be created in less than two hours with the accuracy of 1/10000 of flying height (Krzystek, 1991). Characteristic features such as break lines, boundary areas, and abrupt changes still are digitized manually. In some DEM packages digitized points can be displayed on the stereo imagery for visual checking and editing. Contour lines can also be generated and superimposed on the stereo display for the visual checking.

In any aerial triangulation process, the image coordinates of all tie, control, and check points appearing on all photographs are measured and then a least squares bundle adjustment is performed. This process ultimately provides exterior orientation parameters for all photographs and three-dimensional coordinates for all measured object points. Until recently, all photo measurement was done manually. Furthermore, the block adjustment was a completely separate step.

New advances in digital Photogrammetry permit automatic tie point extraction using image-matching techniques to automate the point transfer and the point mensuration procedures. Automatic Aerial Triangulation (AAT) is already in production rather successfully. The AAT solution has reached the accuracy level of a conventional

aerial triangulation. It has been proven, that the AAT solution is much more economical than a conventional one. However, like any new products, AAT systems need to be improved to fit increasing demands of the users (Madani, 2001).

In addition, innovative technologies like GPS/INS are more and more challenging the business of aerial triangulation, thus they compete with the next generation of AAT systems. Today, about 30 % of aerial photographs are taken with cameras assisted with GPS systems.

Automatic feature extraction is one of the most difficult tasks in digital Photogrammetry. Artificial intelligence and pattern recognition may provide some help to analyze this process. Extraction of linear features and building extraction are somehow automated. An example of this approach might be in the extraction of road networks. Edges can be extracted from the imagery using segmentation operators, and potential road segments are inferred from parallel lines that are separated by an estimate of road width.

### **3.6 SATELLITE PHOTOGRAMMETRY AND SOFTWARE USED**

A clear-cut distinction between satellite and aerial photogrammetric methodology is gone. In the past, aerial imagery was subjected to rigorous photogrammetric processing while satellite imagery, being of only mid to low resolution and typically nadir looking, required much less sophisticated processing.

Similarly, applications for aerial and satellite images once were distinctively different. Aerial imagery was collected and processed mainly for mapping or other applications that require high metric accuracy, such as digital elevation model (DEM)

extraction. Commercial satellite imagery was confined to remote sensing applications and low resolution/low-accuracy resource mapping.

Everything changed with Space Imaging's September 1999 IKONOS satellite launch, and later with DigitalGlobe's QuickBird and ORBIMAGE's OrbView-3 high-resolution satellites, which collect imagery at 0.82 meters, 0.61 meters and 1 meter GSD at nadir, respectively. Similar to aerial imagery, rigorous photogrammetric processing methods, such as block adjustment used to solve aerial blocks totaling hundreds or even thousands of images, are routinely being applied to high-resolution satellite image blocks. High-resolution satellite image camera models have been implemented and are supported by most commercial photogram-metric software vendors such as BAE Systems, PCI Geomatics, Intergraph Z/I and others.

High-resolution satellite imagery, because of its accessibility to sophisticated photogrammetric processing methods, photogrammetric software compatibility, and, most importantly, excellent metric accuracy characteristics, has been increasingly encroaching on traditional aerial territories such as mapping and DEM extraction. Aerial imagery, on the other hand, is being pushed into extremely high-resolution/accuracy applications, such as high-resolution orthos and civil engineering projects.

In addition, there has been movement in the opposite direction. With the advent of wide-area digital aerial sensors with multispectral capabilities, such as the Leica ADS-30 and Intergraph Z/I DMC, aerial imagery is being collected for remote sensing applications—an area previously reserved solely for satellite imagery. More and more, the choice between satellite and aerial solutions is being decided on the basis of resolution, attainable accuracy, imagery accessibility, timeliness and price.



Factors such as software compatibility and rigorousness of photogrammetric processing are no longer relevant.

Apart from these there are some tools of software used such as;

1. ERDAS Imagine:- Orthobase
2. PCI Geomatica:- Ortho Engine
3. ENVI : - DEM Extraction Wizard
4. BAE Systems
5. Intergraph Z/I
6. LPS (Lieca photogrammetric solution)
7. AutoCAD

For any software to generate 3D model it require the information about the camera (Aerial Photogrammetry) or sensors (satellite Photogrammetry). In satellite Photogrammetry RPC file is used for information about the camera and sensors used to take the image. In the next section information about the RPC file is discussed.

### **3.7 DESCRIPTION OF RPC FILE**

Rational Polynomial Camera (RPC) models have become the replacement model of choice for a number of high resolution satellite imagery providers. RPCs provide a simple, efficient, and accurate representation of the camera object-image geometry and allow the end user to perform full photogrammetric processing of satellite imagery including block adjustment, 3D feature extraction and orthorectification. For this study I have used the IKONOS satellite image. The IKONOS RPC model is

### 3.8 IKONOS RPC Model

IKONOS RPCs, comprising 78 rational polynomial coefficients, {c1...c20, d2...d20, e1...e20, f2...f20} alongside 10 scale and offset factors, are provided by Space Imaging with Geo Ortho Kit and stereo image products. They are generated in the Space Imaging ground station by fitting the RPCs to the physical camera model. The RPC functional model is a ratio of two cubic polynomials of object space coordinates, and as such provides a functional relationship between the object space ( $\phi, \lambda, h$ ) coordinates and the image space ( $L, S$ ) coordinates. Separate rational functions are provided for mapping the object space coordinates to line and sample coordinates, respectively. To improve numerical precision, image and object space coordinates are normalized to  $\langle -1, +1 \rangle$  range by applying the offsets and the scale factors as shown below

$$U = \frac{(\phi - \phi_0)}{\phi_s}, V = \frac{(\lambda - \lambda_0)}{\lambda_s}, W = \frac{(h - h_0)}{h_s}, X = \frac{(S - S_0)}{S_s}, Y = \frac{(L - L_0)}{L_s} \dots\dots\dots(1).$$

where  $\phi$  is geodetic latitude,  $\lambda$  is geodetic longitude,  $h$  is height above the ellipsoid,  $S$  and  $L$  are the image sample and line coordinates, and  $\phi_0, \lambda_0, h_0, S_0, L_0, \phi_s, \lambda_s, h_s, S_s, L_s$ , are the latitude, longitude, height, sample and line offsets and scale factors. The line and sample rational functions are given in e.g. (Grodecki and Dial, 2003) as

$$Y = \frac{N_L(U, V, W)}{D_L(U, V, W)} = \frac{e^T u}{d^T u}, \text{ and } X = \frac{N_s(U, V, W)}{D_s(U, V, W)} = \frac{e^T u}{f^T u} \dots\dots\dots(2)$$

Where,

$$N_L(U, V, W) = c_1 + c_2V + c_3U + c_4W + c_5VU + c_6VW + c_7VW + c_8V^2 + c_9U^2 + c_{10}W^2 + c_{11}UVW + c_{12}V^3 + c_{13}VU^2 + c_{14}VW^2 + c_{15}V^2U + c_{16}U^3 + c_{17}UW^2 + c_{18}V^2W + c_{19}U^2W + c_{20}W^3 = e^T u$$

$$D_L(U, V, W) = 1 + d_2V + d_3U + d_4W + d_5VU + d_6VW + d_7VW + d_8V^2 + d_9U^2 + d_{10}W^2 + d_{11}UVW + d_{12}V^3 + d_{13}VU^2 + d_{14}VW^2 + d_{15}V^2U + d_{16}U^3 + d_{17}UW^2 + d_{18}V^2W + d_{19}U^2W + d_{20}W^3 = d^T u$$

$$N_x(U, V, W) = e_1 + e_2V + e_3U + e_4W + e_5VU + e_6VW + e_7VW + e_8V^2 + e_9U^2 + e_{10}W^2 \\ + e_{11}UVW + e_{12}V^3 + e_{13}VU^2 + e_{14}VW^2 + e_{15}V^2U + e_{16}U^3 + e_{17}UW^2 \\ + e_{18}V^2W + e_{19}U^2W + e_{20}W^3 = e^T u$$

$$D_x(U, V, W) = 1 + f_2V + f_3U + f_4W + f_5VU + f_6VW + f_7VW + f_8V^2 + f_9U^2 + f_{10}W^2 \\ + f_{11}UVW + f_{12}V^3 + f_{13}VU^2 + f_{14}VW^2 + f_{15}V^2U + f_{16}U^3 + f_{17}UW^2 \\ + f_{18}V^2W + f_{19}U^2W + f_{20}W^3 = f^T u$$

With,

$$u = [1 \quad V \quad U \quad W \quad VU \quad VW \quad V^2 \quad U^2 \quad W^2 \quad UVW \quad V^3 \quad VU^2 \quad VW^2 \quad V^2U \quad U^3 \quad UW^2 \\ V^2W \quad U^2W \quad W^3]^T$$

$$c = [c_1 \quad c_2 \quad \dots \quad c_{20}]^T$$

$$d = [d_1 \quad d_2 \quad \dots \quad d_{20}]^T$$

$$e = [e_1 \quad e_2 \quad \dots \quad e_{20}]^T$$

$$f = [f_1 \quad f_2 \quad \dots \quad f_{20}]^T$$

## DATA USED AND METHODOLOGY

## 4.1 DATA USED

IKONOS stereo satellite data from latitude  $73^{\circ} 26' 51.51''\text{N}$  to  $73^{\circ} 31' 3.41''\text{N}$  to longitude  $18^{\circ} 22' 53.22''\text{E}$  to  $18^{\circ} 26' 27.34''\text{E}$  acquired on 24<sup>th</sup> May 2006 was used for the study (Figure). Study area located in the western mountain ranges of India, at an altitude of 500-1500 m above sea level.

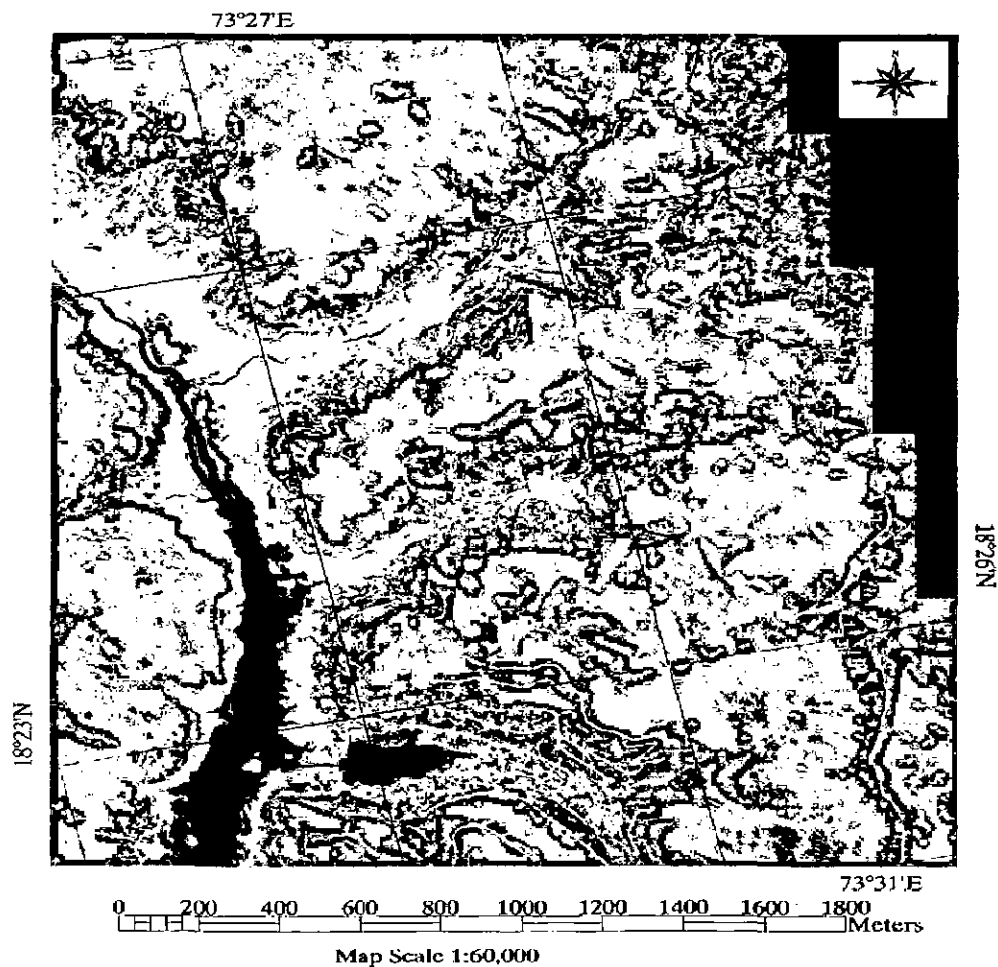


Figure 4.1 : IKONOS Imagery of Study Area

#### 4.2 WORK FLOW DIAGRAM OF GENERATION OF DEM WITH RPC

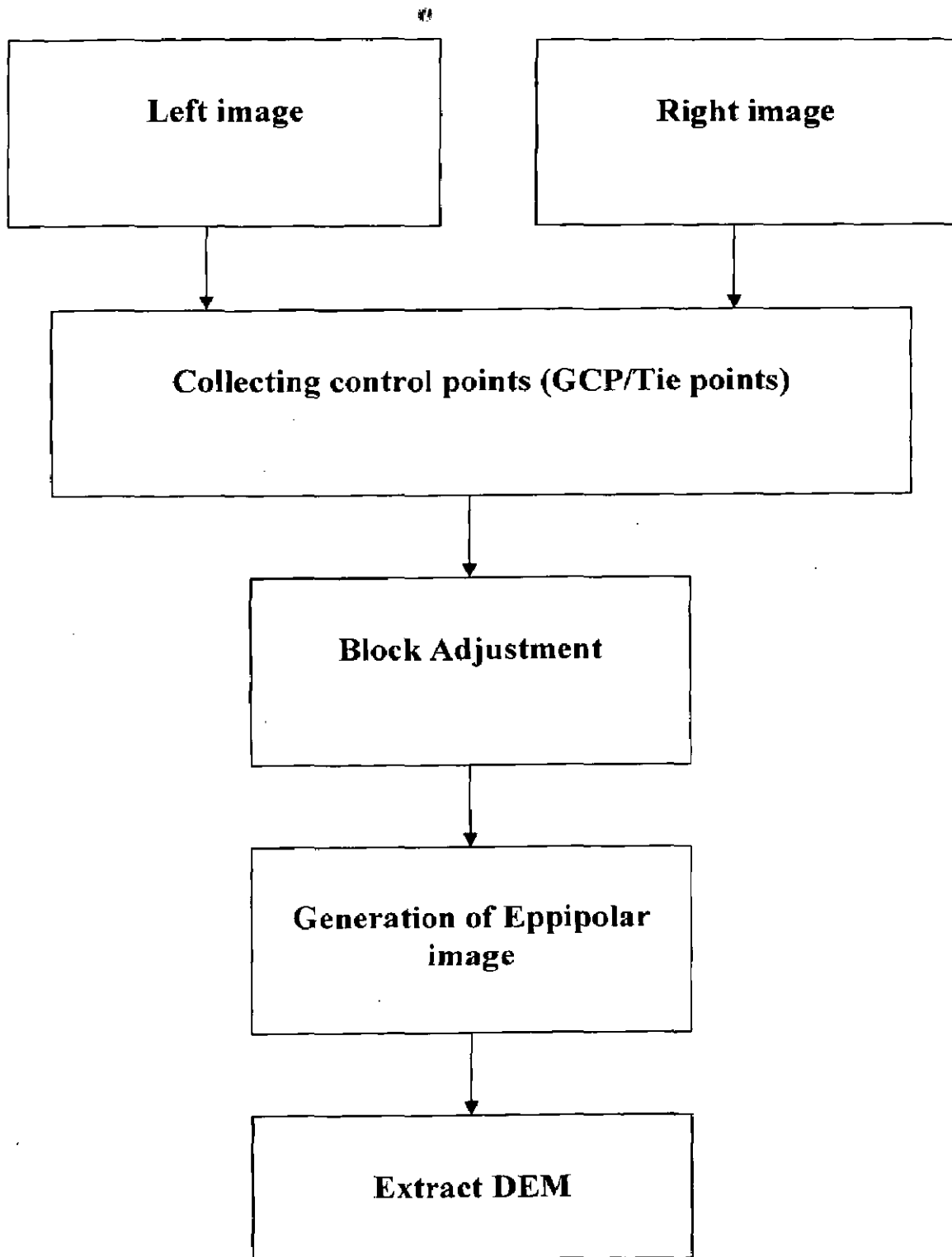
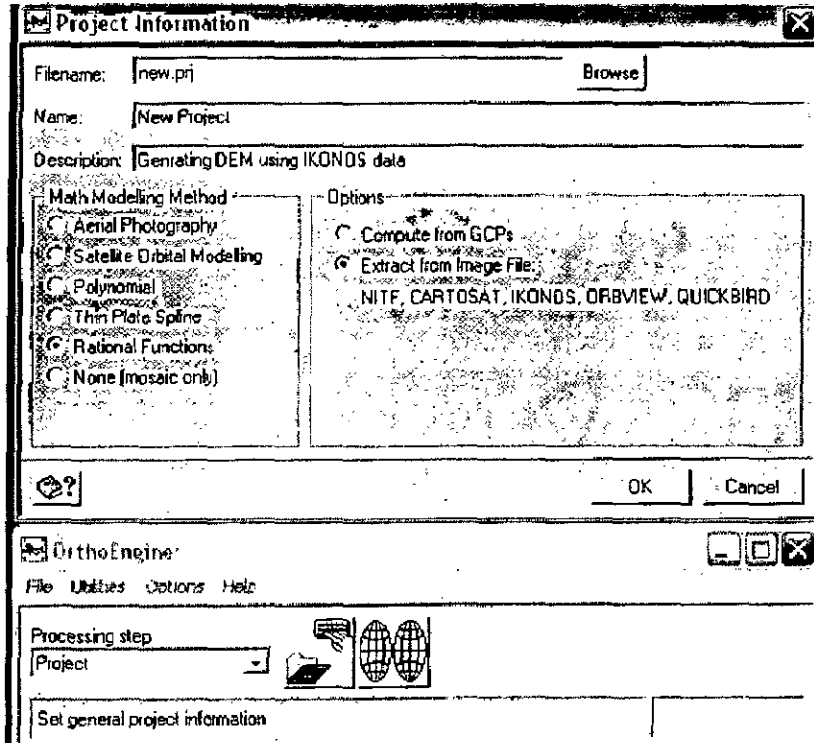


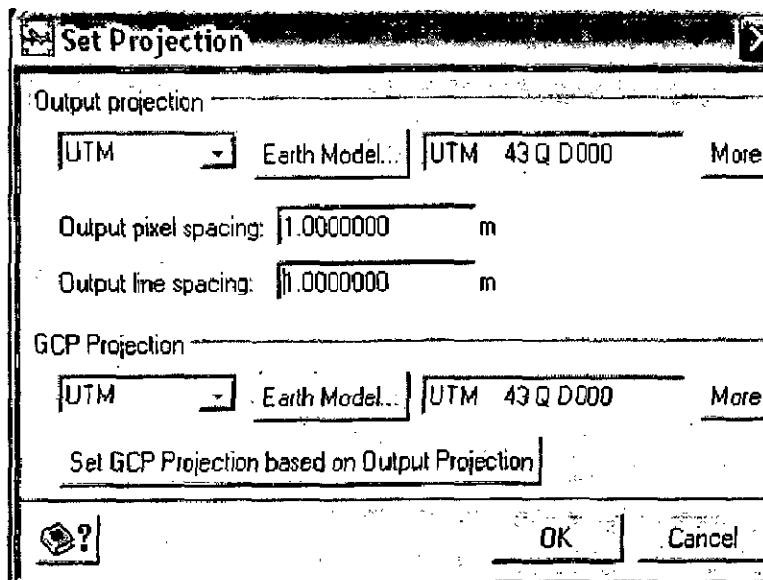
Figure 4.2 Work Flow Diagram of Generation of DEM with RPC

### 4.3 GENERATING DEM USING GEOMATICA 10.0

Step 1 Create a new project and give all information shown in fig.



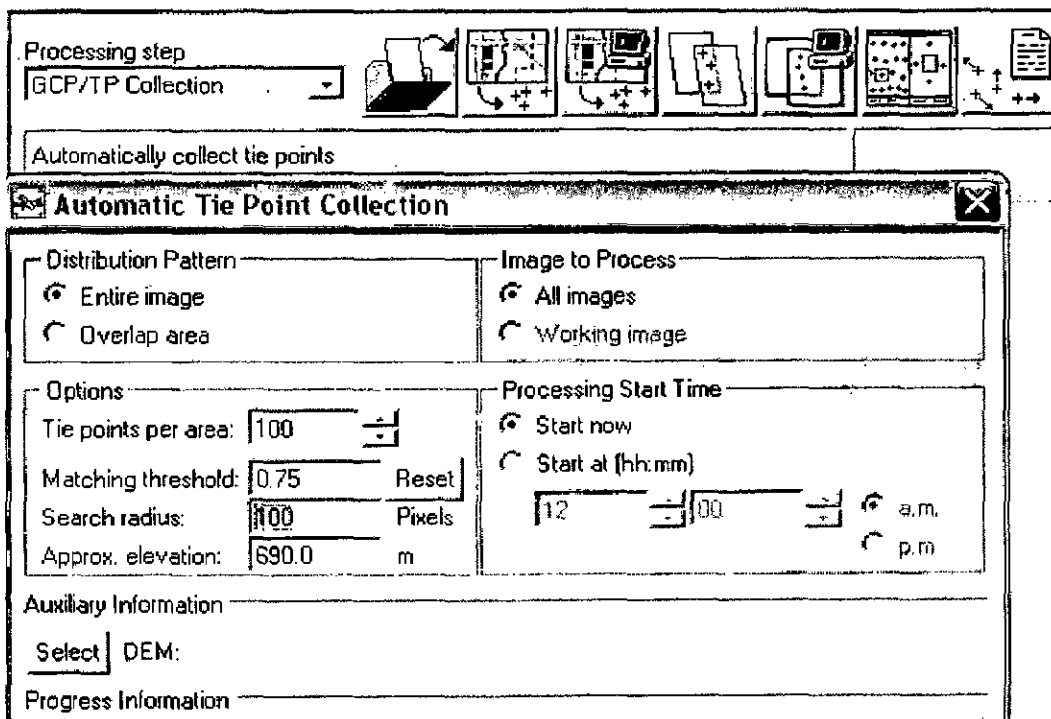
Step 2 set projection



### Step 3 Data Input (open both image of stereo pair left and right)

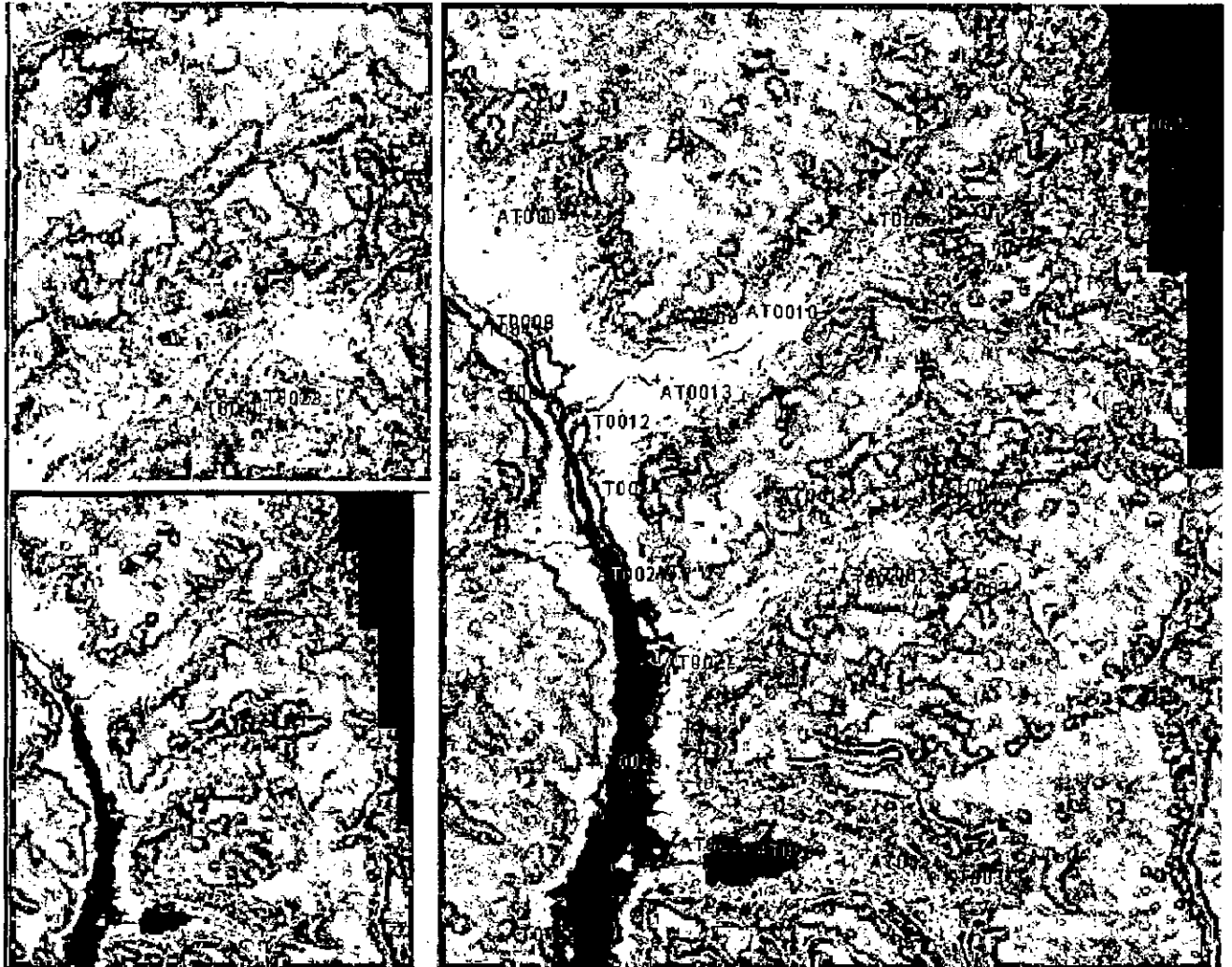
### Step 4 TP collection

There are two method one automatic collect TP another one is manually collection. Collection depend on the need of the project



**Tie point:** - A tie point is a feature that we can clearly identify in two or more images and that we can select as a reference point. Tie points do not have known ground coordinates, but we can use them to extend ground control over areas where you do not have ground control points (GCPs). Used in rigorous models such as Aerial Photography and Satellite Orbital (high and low resolution) math models, tie points identify how the images in your project relate to each other. In a project using the Rational Functions math model where we have imported the polynomial coefficients distributed with the data, we

can collect tie points and ground control points to compute a transformation to improve the fit between the images. Fig show the tie points



**Step 6** creating eppipolar image.

Eppipolar images are stereo pairs that are reprojected so that the left and right images have a common orientation, and matching features between the images appear along a common x axis. Using eppipolar images increases the speed of the correlation process and reduces the possibility of incorrect matches



Epipolar selection:

User select  Minimum percentage overlap:

Left Image

```
po_2610900_rgb_0000020100;.I:\3\
po_2610900_rgb_0020000100;.I:\3\
```

Channel:  Channels   
 All

Right Image

```
po_2610900_rgb_0020000100;.I:\3\
```

Channel:  Channels   
 All

Epipolar pairs:

Number	Select	Left File	Right File	Left Channels	Right Channels
1	<input checked="" type="checkbox"/>	2610900_rgb_0000020100	2610900_rgb_0020000100	All	All

Options

Working cache (MB):

Down sample factor:

Down sample filter:

Processing Start Time

Start now

Start at (hh:mm)

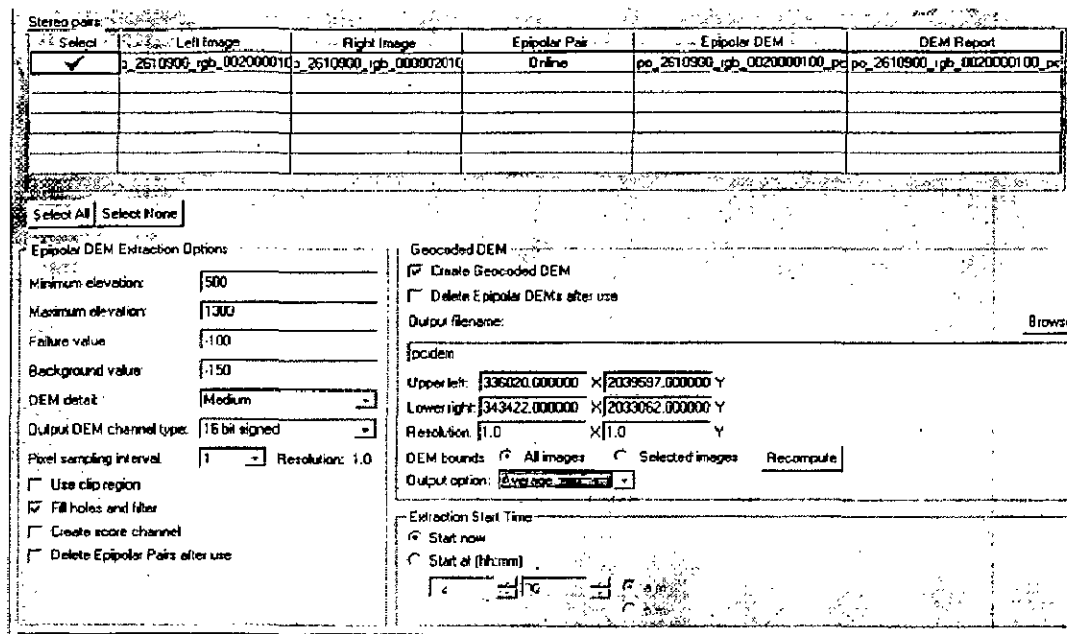
a.m.  
 p.m.

### Step 7 Extracting a digital elevation model from epipolar pairs

The process of generating a digital elevation model (DEM) consists of several steps:

Convert the raw images into epipolar pairs.

Epipolar images are stereo pairs that are reprojected so that the left and right images have a common orientation, and matching features between the images appear along a common x axis.



Extract DEMs from the overlap between the epipolar pairs.

The resulting DEMs are called epipolar DEMs. They are not georeferenced at this stage.

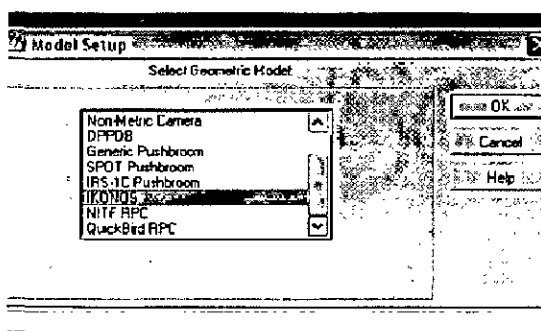
Geocode the epipolar DEMs and stitch them together to form one DEM.

The result is one DEM reprojected to the ground coordinate system

#### 4.4 GENERATING DEM USING ERDAR 8.6

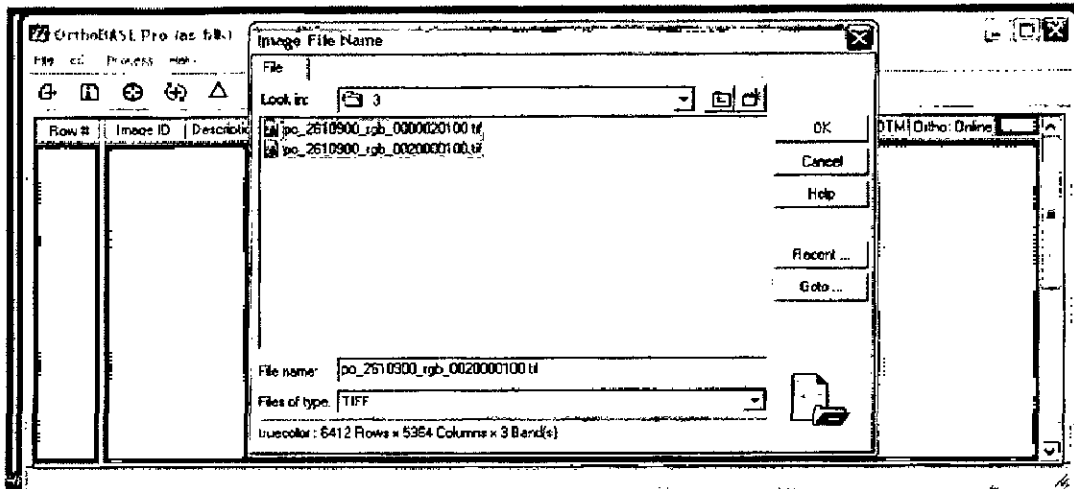
**Step 1** Create a new orthobase project

**Step 2.**Select geometric model



**Step 3** Set the projection system for reference

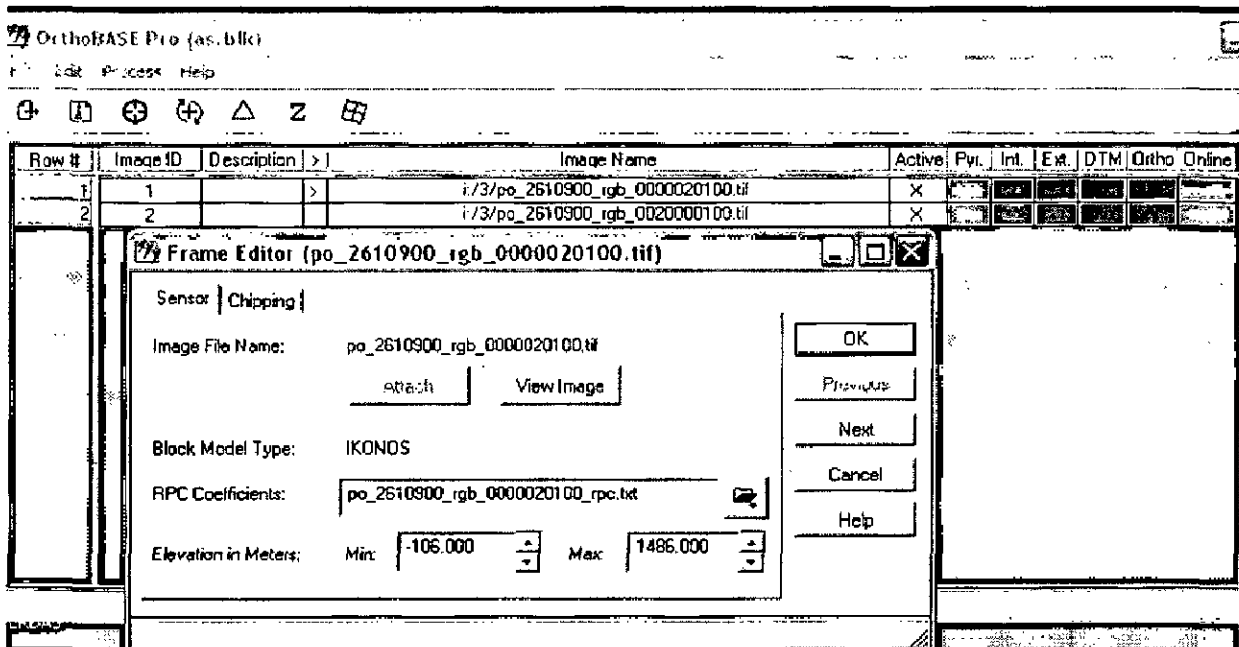
**Step 4.** Add frame to the list ... these frames are the satellite images (stereo pairs)



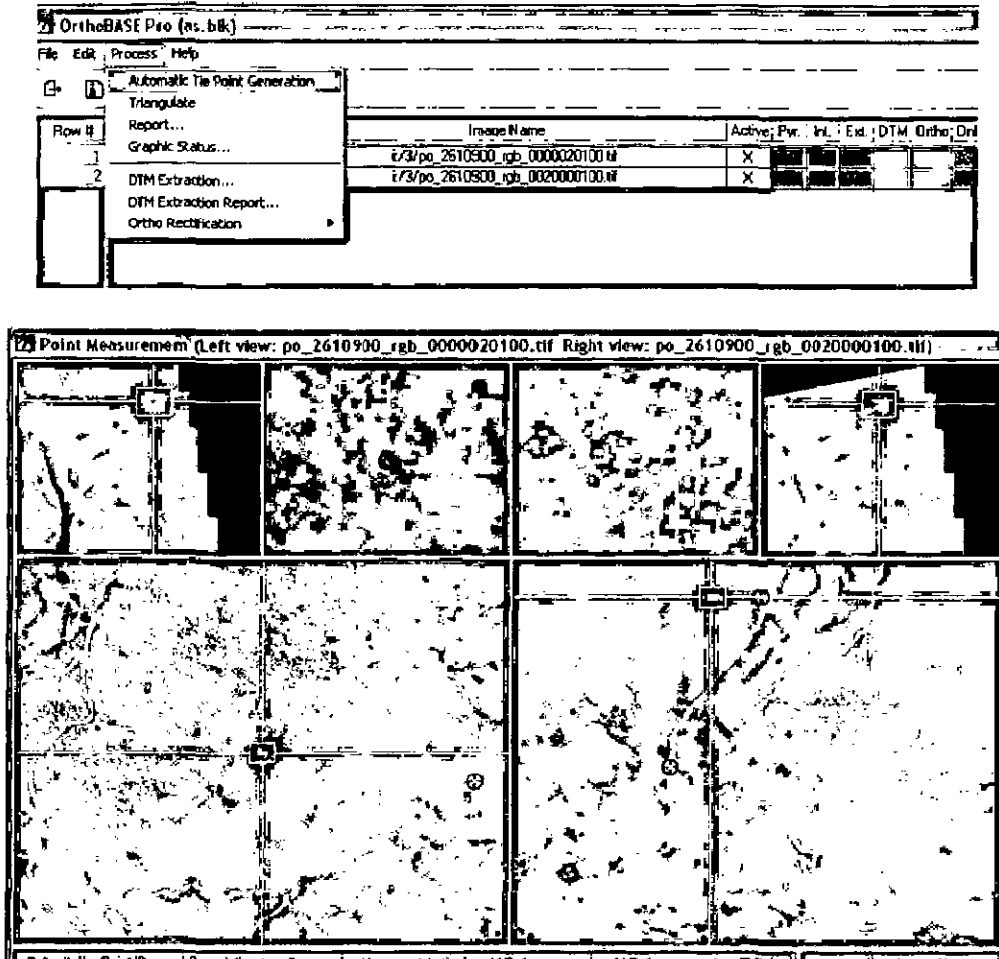
**Step 5.** Open the frame editor to view and edit the properties associated with an image file added to the project file. This includes sensor model information defining the internal and external properties associated with the camera or satellite.

This dialog allows us to set the interior orientation and exterior orientation properties of the camera used to capture the data used in our project

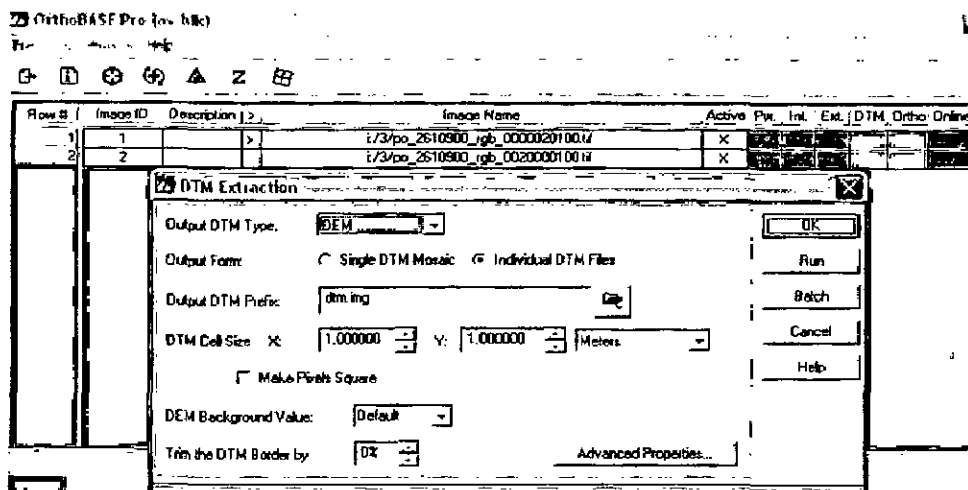
This information is given by the RPC file associated with the image



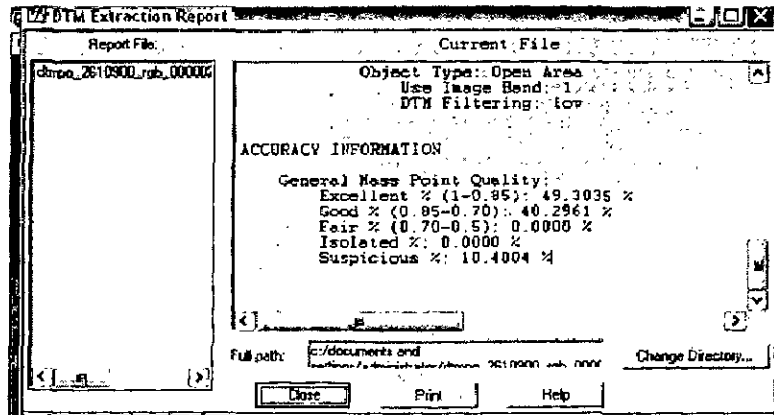
## Step 6 Generation of automatic tie points



## STEP 7 DTM extraction

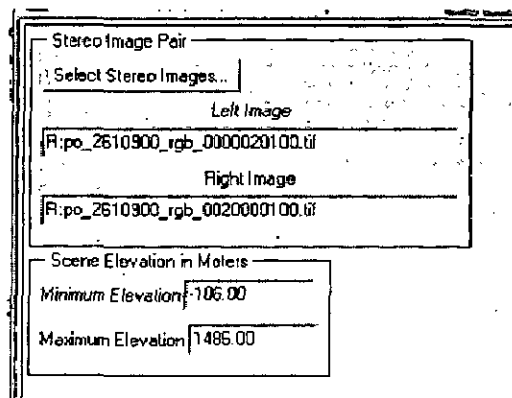


## Step 8 Report

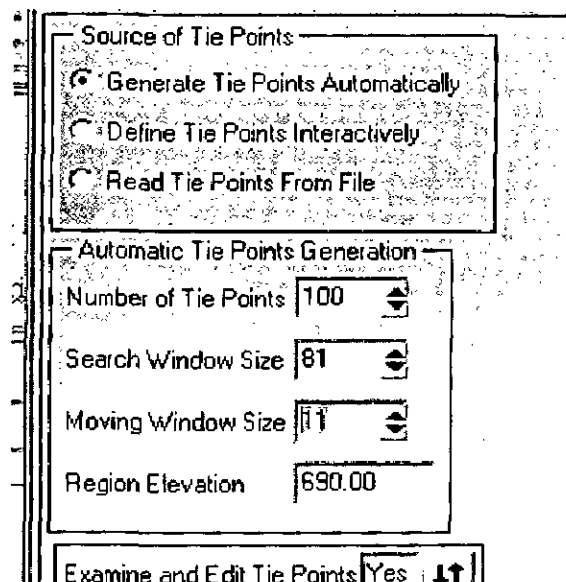


## 4.5 GENERATING DEM USING ENVI 4.3 10.0

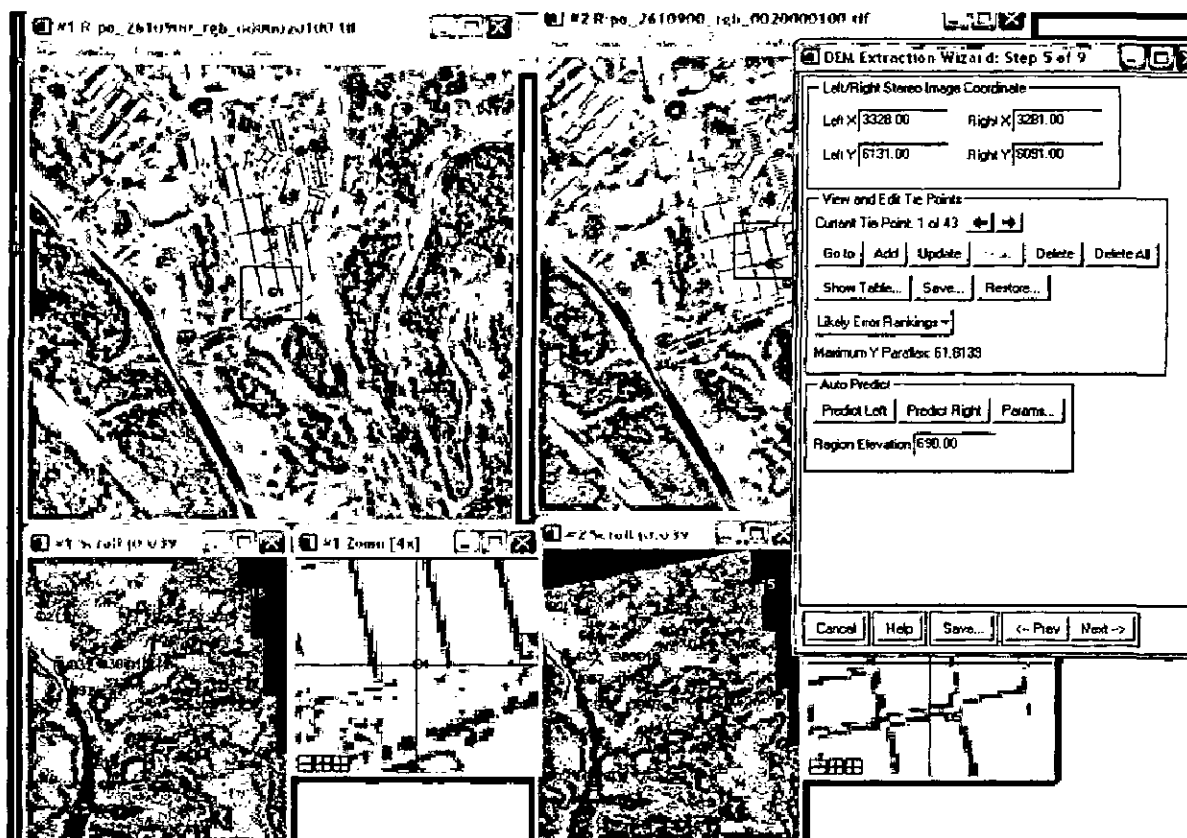
### Step 1 Select stereo pair



### Step 2. Generate tie points.



### Step 3 Tie points can be editing



### Step 4 Generating eppiporar image

Using the tie points, ENVI will calculate the eppipolar geometry and eppipolar images that are used to extract the DEM. These eppipolar images describe the relationship between the pixels in the stereo pair and they can be viewed in 3D using anaglyph glasses.

### Step 5 Output projection and map extant

DEM Extraction Wizard allows us to set parameters for the DEM output projection and map extents. We have the option to change parameters such as the output projection type, pixel size, or output image size

Output Projection and Map Extent

Upper Left Corner Coordinate

Proj: UTM, Zone 43 North  
Datum: WGS-84

336007.2285 E Change Proj...

2039665.7407 N Units: Meters

X Pixel Size 1.00000000 Meters

Y Pixel Size 1.00000000 Meters

Output X Size 7444 pixels

Output Y Size 6640 pixels

Options

**Step 6. Pass the DEM extraction parameter**

DEM Extraction Wizard allows us to specify the parameters for the DEM extraction. Here we can define thresholds, set the size of the area in which we wish to perform image matching, determine the level of terrain detail, and specify where to save our DEM result.

DEM Extraction Parameters

Minimum Correlation 0.80

Background Value -999.00

Edge Trimming 0.00

Moving Window Size 5 x 5

Terrain Relief High

Terrain Detail Level 1 (min)

DEM Result

Output Data Type Integer

Output Result to  File  Memory

Output DEM Filename Choose

demervi

**Step 7 Generate DEM**

**5.1 RESULTS AND ANALYSIS**

**5.1.1 Analysis of DEM Generated by Different Softwares**

As mentioned in last chapter for the present study IKONOS data is used to generate DEM using three different photogrammetric modules available in ERDAS imagine 8.6, ENVI 4.3 and Geomatica PCI 10.0 software. The DEM generated from these three modules are in Fig 5.1(a) to (c) as shown below:



Fig 5.1(a): DEM using ERDAS Imagine 8.6



Fig 5.1(b): DEM using ENVI 4.3



Fig 5.1(c): DEM using Geomatica PCI 10.0



The basic statistics of the DEM generated using different software's are listed in Table 5.1. The minimum and maximum elevation in the DEM with their mean is compared in the this.

Table 5.1: Basic Statistics

DEM source	Minimum	Maximum	Mean
ENVI	484	1041	670
ERDAS	540	1024	690
Geomatica	624	1226	780

The results given by ERDAS and ENVI are slightly difference from the results given by Geomatica; this is because during the DEM generation process, the initial values of minimum and maximum elevation values shown in Table 5.1 corresponding to Geomatica is provided by user. Taking these initial elevation values, Geomatica proceed further for DEM generation. In case of ENVI, it takes the height offset and scale factors from the RPC file and maximum scene elevation in generation of DEM..

### 5.1.2 Analysis of Tie Point Generated through Photogrammetric Software

For any DEM generation the most important factor is considering tie points. Accuracy of tie points is very important in the process of DEM generation. When generating DEM using satellite Photogrammetry it create tie points on both the stereo image. RPC file that contain all the information about the geometry of camera is used to create the tie points. Tie point can be created manually or automatic. In this study it used automatic tie point collection.

In the process of tie point collection three parameters should be set as discussed below.

### **1. No. of point per image:**

It depends on the need of the study and the study area. If there is more undulating terrain it needs more tie points. But with the increase in tie points per image, total number of collected tie points is increased but accuracy of these tie point is decreased.

### **2. Search window size:**

The search window is a defined subset of the image, within which the smaller moving window scans to find a topographic feature match for a tie point placement. This value depends upon the correctness of map, RPC, RSM, or pseudo map information for the base and warp image, and it also depends on the roughness of terrain

### **3. Correlation factor:**

Correlation factor or threshold value is the most important factor in generation of auto tie point. Its value varies between 0 to 1 where 0 means no matching and 1 means perfect match. For better correlation this value should be near to 1.

When we increase the correlation factor we get less number of points. Sometime no point may be match with higher factor. The ideal value to work is 0.75 to 0.90.

Even taking the all factor into account we get some points having more RMSE for the study purpose it generate auto tie points and then remove the points having RSME less so the remaining points have the higher RSME from that we can conclude some interesting results, in Fig 5.1 show complete tie points and in Fig 5.2 show the points having higher RSME value or not so accurate.

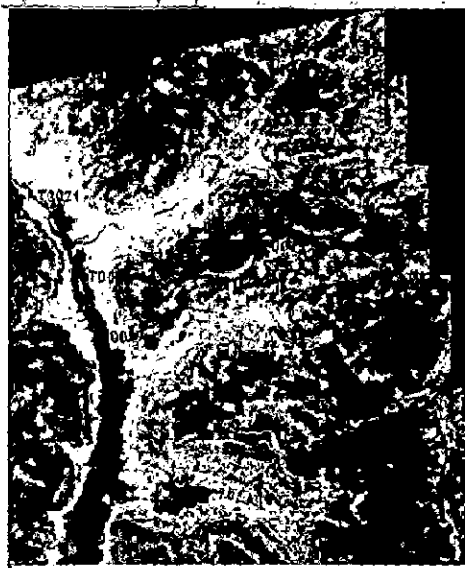


Fig 5.2 All Tie Points



Fig 5.3 Erroneous Tie Points

In this study these three factors named as *no. of points per image*, *window size* and *correlation coefficient* which influences the accuracy of the tie points. Out of these three factors, two remains constant and only one factor varies during tie point generation and results of this process is given below.

1) No. of points per image =100

Window size = 100

Correlation factor	0.5	0.6	0.7	0.75	0.8	0.85	0.9
Points collected	84	82	69	51	40	23	5
Allowable points (error <1RMSE)	12	13	17	19	20	18	4

2) No. of points per image =200

Window size = 200

Correlation factor	0.5	0.6	0.7	0.75	0.8	0.85	0.9
Points collected	176	152	132	91	82	34	16
Allowable points (error <1 RMSE)	32	41	42	37	39	29	13

3) No. of points per image =400

Window size = 400

Correlation factor	0.5	0.6	0.7	0.75	0.8	0.85	0.9
Points collected	302	278	240	146	120	103	24
Allowable points (error <1 RMSE)	11	30	32	38	40	42	18

4) No. of points per image =400

Window size = 100

Correlation factor	0.5	0.6	0.7	0.75	0.8	0.85	0.9
Points collected	290	270	169	151	80	43	21
Allowable points (error <1 RMSE)	11	18	17	38	42	18	15

5) no of point =100

Correlation factor = 0.8

Window size	100	200	300	400
No. of points collected	40	49	58	62
Allowable points ( error<1 RMSE)	20	17	16	19

From the above tables, it can be understood that the entire 3 factor has been taken into account to generate tie points and same things are helpful for the comparison of accurate tie points. But the most important factor is correlation coefficient. It matches the feature

of the tie point in both the image so that higher the correlation factors higher the accuracy of the point. But there are also some limitations such as after certain increments in correlation coefficient, if it increased then tie points will be decreased. Due to this, accurate tie points will be less than the accurate points collected when correlation coefficient is less as shown in above table.

### 5.1.3 Comparison of Elevation between Three Software

As shown in graph ERDAS and ENVI contain almost same elevation points where in PCI elevation value is higher than the other two.

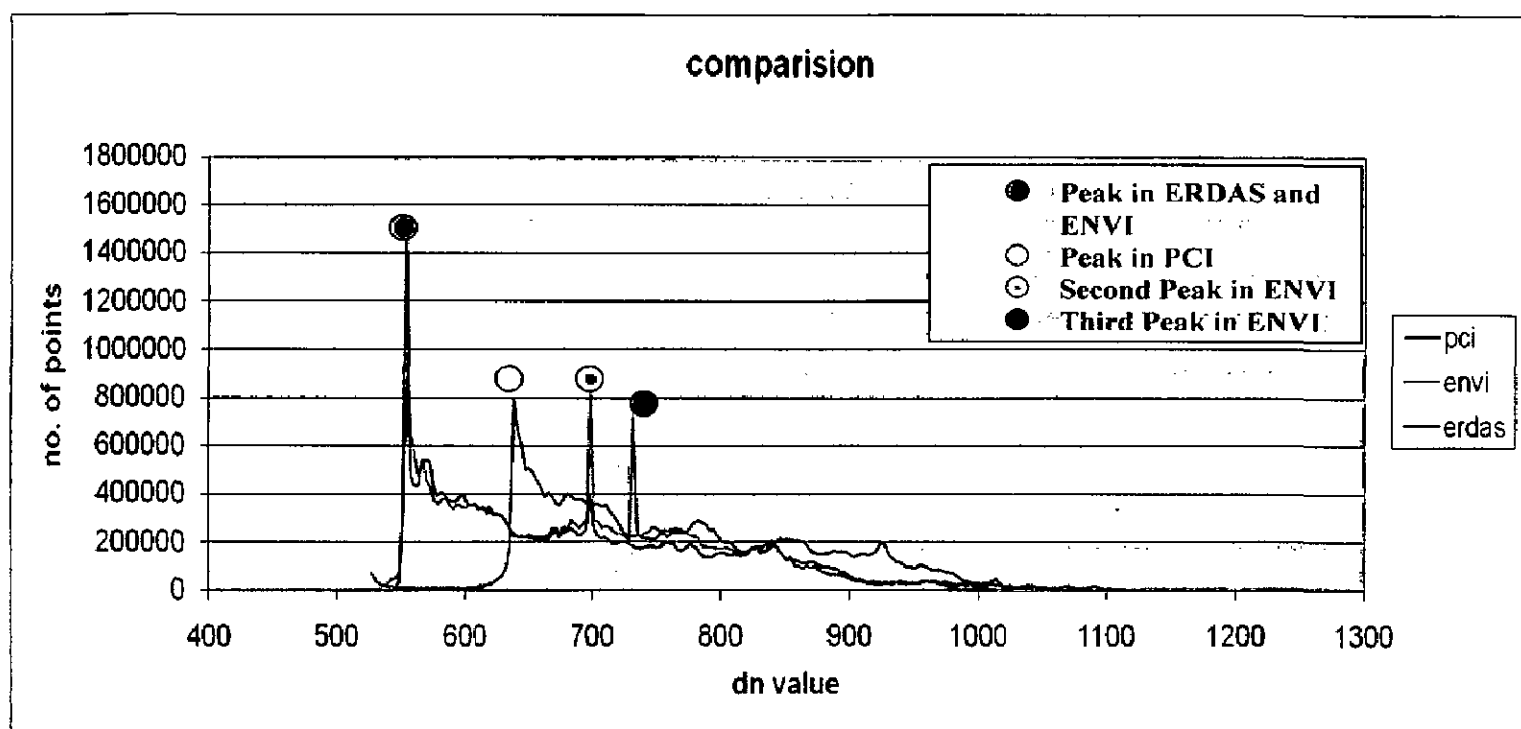


Fig 5.4 Graph between Elevation and Number of Points

The graph show highest number of points with the same elevation is in the water bodies that mean in water bodies the difference in elevation is not high. From the figure below we can see the elevation of water bodies in these three software.

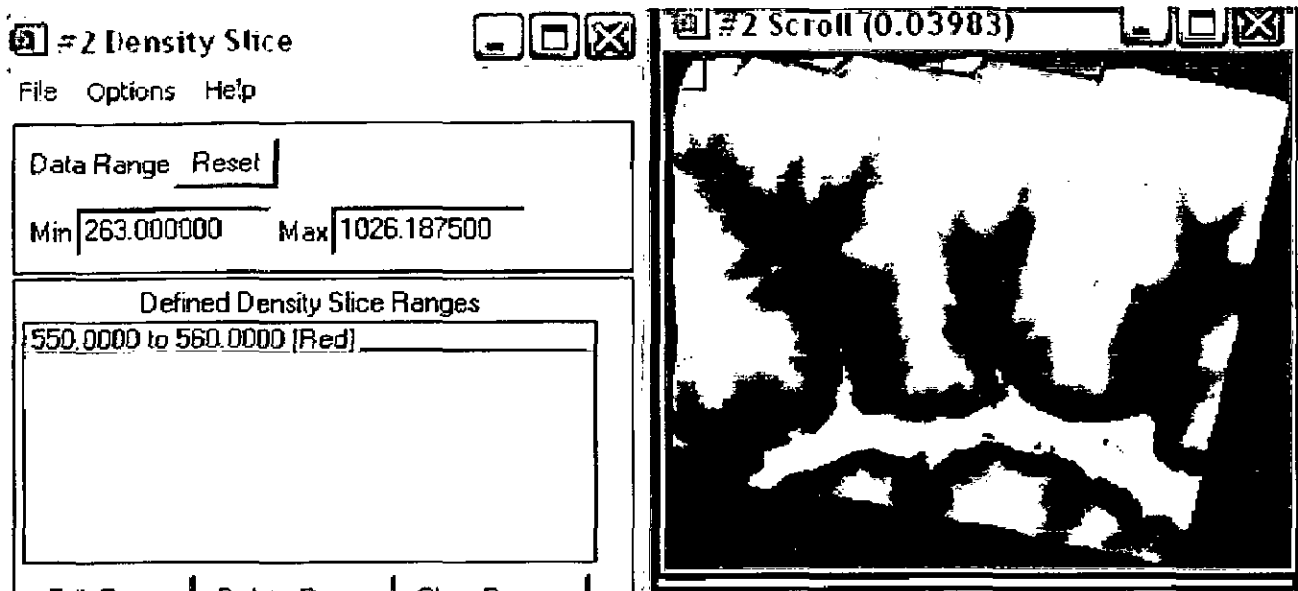


Fig 5.5(a) Water Bodies in ERDAS Imagine

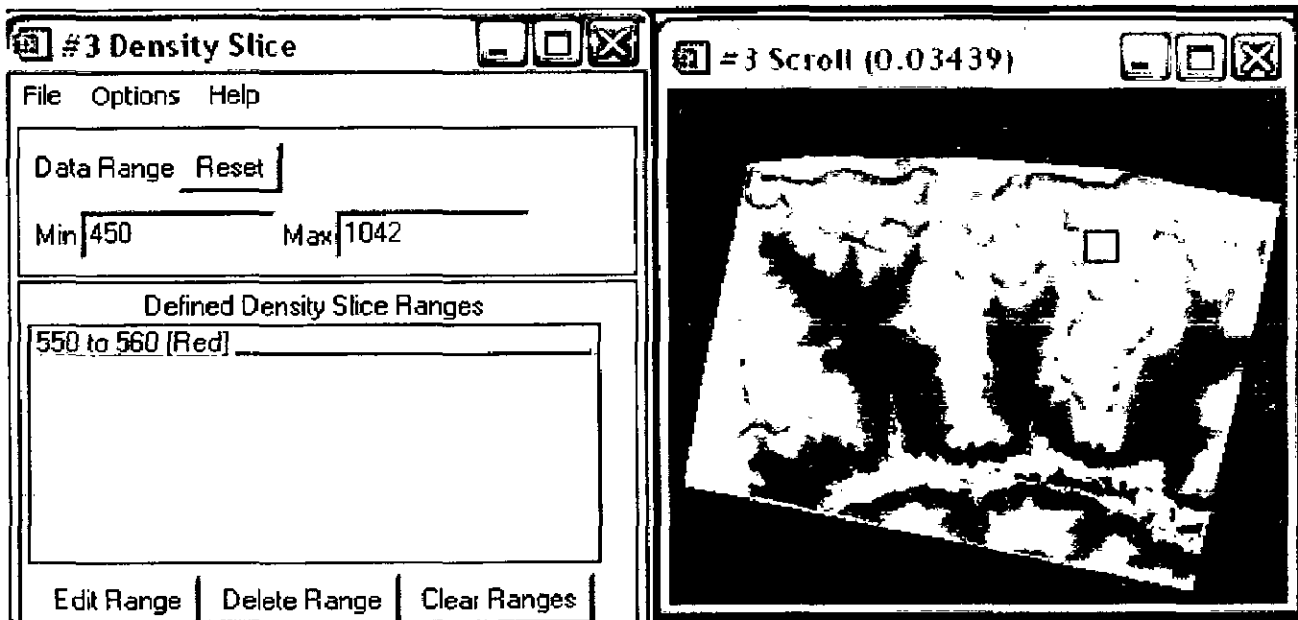


Fig 5.5(b) Water Bodies in ENVI

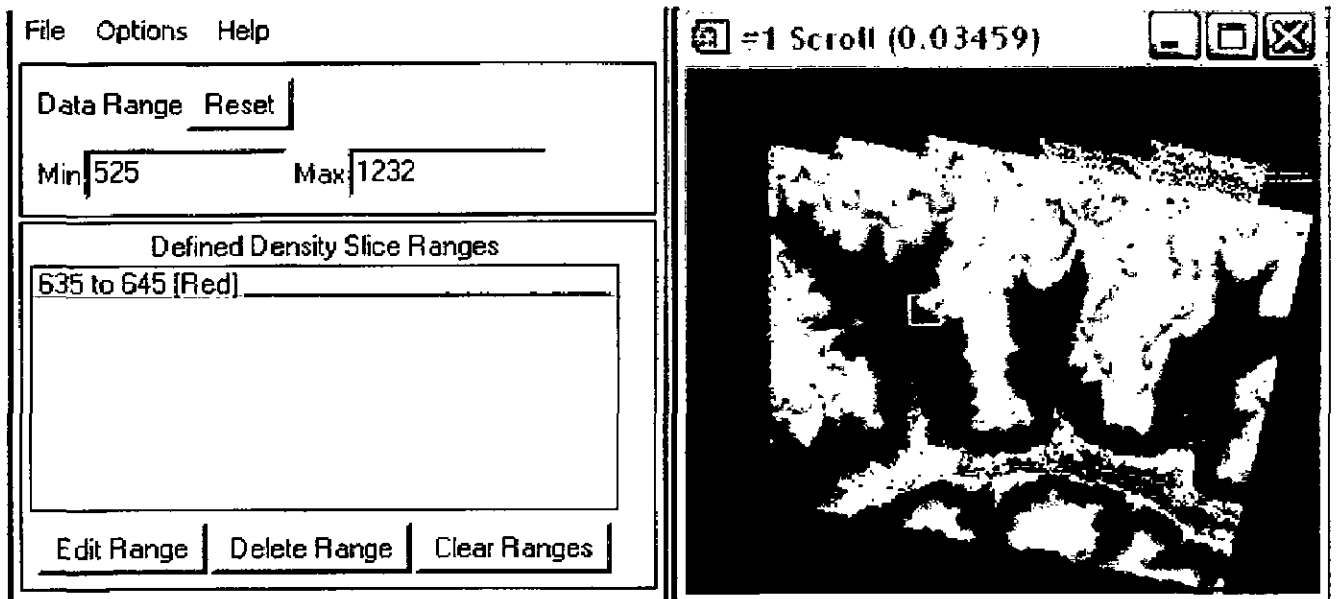


Fig 5.5(c) Water Bodies in PCI Geomatica

After Generating DEM counter lines is shown for better understanding of the result. There contour interval is 50 in each of the DEM. Next figures showing the contour line of all the three DEM generated by different software



Fig 5.6 Contour Lines in ENVI

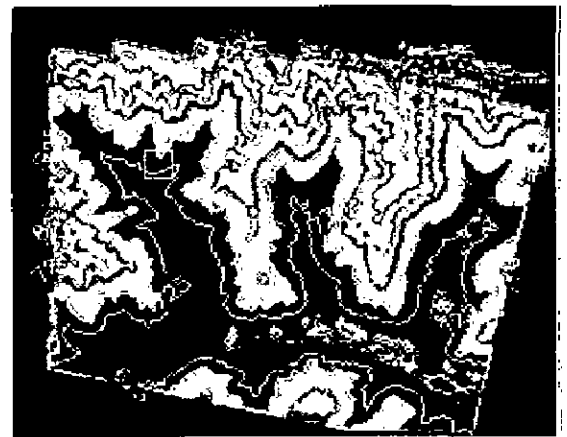


Fig 5.7 Contour Lines in PCI



Fig 5.8 Contour Lines in ERDAS

Color of contour is shown in below fig 5.9

Defined Contour Levels	
[525]	"575" (Solid:Red:1)
[575]	"625" (Solid:Green:1)
[625]	"675" (Solid:Blue:1)
[675]	"725" (Solid:Cyan:1)
[735]	"775" (Solid:Magenta:1)
[775]	"825" (Solid:Maroon:1)
[825]	"875" (Solid:Sea Green:1)
[875]	"925" (Solid:Coral:1)
[925]	"975" (Solid:Aquamarine:1)
[975]	"1025" (Solid:Thistle:1)
[1025]	"1075" (Solid:Sienna:1)
[1075]	"1125" (Solid:Orchid:1)
[1125]	"1175" (Solid:Red1:1)
[1175]	"1225" (Solid:Red3:1)

Fig 5.9 Contour Interval

From the fig 5.4 there are two peaks in ENVI which are not available in other two software as shown in fig 5.10 and fig 5.11.



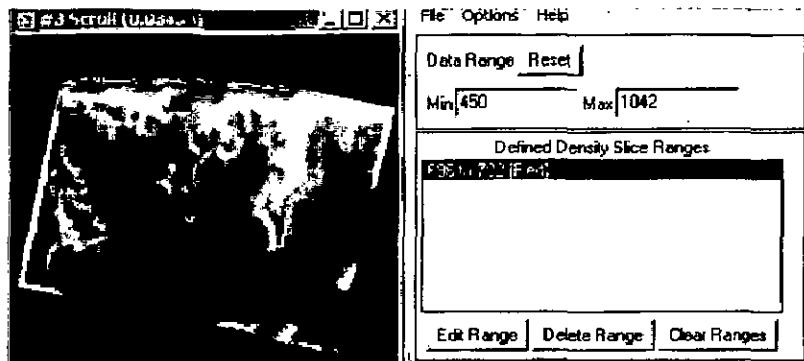


Fig 5.10 Density slice of peak in ENVI

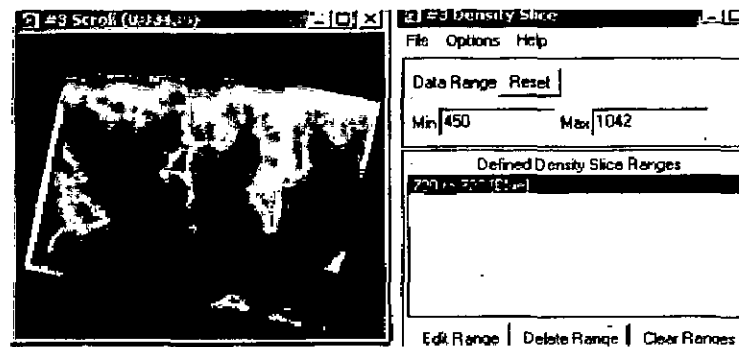


Fig 5.11 Density slice of next peak in ENVI

**Analysis:** Figure 5.4 show the graph between total no of point and elevation. From the graph we can easily seen that there are some peaks in the in each DEM and highest peak is the elevation of water body that has been shown in fig 5.5 (a,b,c). In the ERDAS and ENVI graph is comparatively similar to each other but in PCI graph is different.

Contour line has been generated for each DEM from that we can easily say that ERDAS and ENVI have contour interval equal to each other. In ENVI there are two peaks extra which indicate the change in texture. That means changing in texture can be best identify in ENVI.

## 5.2 RESULT AND CONCLUSION

Following conclusions are made from the present study:

- Automatic Tie points having maximum errors are corner points and points near the water surface.
- During the generation of the DEM, boundary of the image should be defined properly so the corner point will not affect the accuracy.
- Elevations of water bodies are different in different software.
- In all three software there is change in the elevation of the water body because of the change of shade in water body. Change of shade is determine in different software is different. That's why when considering the generation of DEM water body should be masked. There is no need to take it in DEM for the better accuracy of DEM
- Tie points per image, Correlation window size and correlation coefficient influence significantly during process of tie point's generation.
- ERDAS and ENVI contain almost same elevation points where in PCI elevation value is higher than the other two.
- The statistical result given by ERDAS and ENVI is approximately same but at the same time result given by Geomatica is different from above mentioned softwares.
- When DEM generated using RPC framework, it provides greater flexibility and enable non technical user to exploit the full potential of high resolution imagery. In the present study also RPC frame work helps a lot during DEM generation process.

### **5.3 FURTHER STUDY RECOMMENDATIONS**

This study can be extended towards the accuracy assessment of generated DEM by different software, as well as different type of data can be used to assessment of the accuracy of particular software for different type of terrain.

## REFERENCES

---

- [1]. Akira Hirano, Roy Welch and Harold Lang, 2003, Mapping from ASTER stereo image data: DEM validation and accuracy assessment, *Journal of P&RS*, 57, pp: 356-370.
- [2]. Aurora Cuartero, A.M.Felicisimo and F.J.Arisa, 2005, Accuracy, Reliability and Depuration of SPOT HRV and Terra STER DEMs, *IEEE Transactions on Geoscience and Remote Sensing*, Vol.43, NO. 2, Feb., pp: 404-407.
- [3]. Baltsavias, E.P., 1996. Digital orthoimages – A powerful tool for the extraction of Spatial- and geo-information, *ISPRS J. Photogram. Remote Sens.*, 51, 63–77, 1996.
- [4]. Bell, J.C., Cunningham, R.L., Havens, M.W., 1992. Calibration and validation of a soil landscape model for predicting soil drainage class. *Soil Sci. Soc. Am. J.* 56, 1860–1866.
- [5]. Bell, J.C., Cunningham, R.L., Havens, M.W., 1994a. Soil drainage class probability mapping using a soil-landscape model. *Soil Sci. Soc. Am. J.* 58, 464–470.
- [6]. Bell, J.C., Thompson, J.A., Butler, C.A., McSweeney, K., 1994b. Modeling soil genesis from a landscape perspective. *Trans. Int. Congress of Soil Science 15th, Acapulco, Mexico. 10–17 July 1994, vol. 6a. ISSS, Vienna, pp. 179–195.*
- [7]. Beven, K. J., and Kirkby, M. J. 1979, A physically based, variable contributing area model of basin hydrology. *Hydrol. Sci. Bull.* 24:43–69.

- [8]. Burrough, P.A. & McDonnell, R.A., 1998, Principles of Geographical Information System, Oxford University Press, Oxford.
- [9]. Carrara, A., Bitelli, G. and Carla, R., 1997, Compression of techniques for generating digital terrain models from contour lines. *Int.J.GIS*, 11 (5), pp.451-473.
- [10]. Carter, J.R. 1988. Digital representations of topographic surface. *Photogrammetric& Engineering and Remote Sensing*, 54, 1 577- 1580.
- [11]. Chadwick, O.A., Chamran, F., Gessler, P.E., 2000. Measurement and modeling of spatially distributed ecological processes in soil landscapes. In: Bell, J.C. \_Ed., *Proceedings of The Second International Conference on Soil Resources*. June 10–12, Minneapolis,
- [12]. Chang, K.-T., Tsai, B.-W., 1991. The effect of DEM resolution on slope and aspect mapping. *Cartogr. Geogr. Inf. Syst.* 18, 69–77.
- [13]. De Bruin, S., Stein, A., 1998. Soil-landscape modeling using fuzzy c-means clustering attribute data derived from a digital elevation model\_DEM.. *Geoderma* 83, 17-33.
- [14]. Day, T. & Muller, J.P., 1988, Quality assessment of digital elevation models produced by automatic stereo-matchers from SPOT image pairs. *Photogrammetric Record*, 12, 797-808.
- [15]. F. Amhar, J. Josef, and C. Ries, The generation of true orthophotos using a 3D building model in conjunction with a conventional DTM. *Int. Archives Photogram. Remote Sens.*, 32(4), 16-22, 1998.

- [16]. Foot, K.E. and Huebner, D.J., 1997, *The Geographers craft*, University of Texas, Austin. <http://www.utexas.edu/depts/grg/gcraft/notes/error/error.html> (Last Accessed 10.12.2004).
- [17]. Gao, J., 1997, Resolution and Accuracy of terrain representation by Grid DEMs at a micro-scale, *Int.J. of GIS*, 11(2), pp:199-212.
- [18]. Gessler, P.E., Moore, I.D., McKenzie, N.J., Ryan, P.J., 1995. Soil-landscape modeling and the spatial prediction of soil attributes. *Int. J. Geogr. Inf. Syst.* 9 4., 421–432.
- [19]. Gruber, U., and Haefner H 1995, *Avalanche Mapping with Satellite Data and a DEM*. *Applied Geography*. Vol. 15, No. 2 p.99-113
- [20]. Gong, J. Li, Z.L., Zhu, Q., Sui, H.H., and Shou, Y. 2000. Effects of various factors on the accuracy of DEMs: an intensive experimental investigation. *PE&RS*, 66(9), pp: 1113-1117.
- [21]. Goodchild, M., Buttenfield, B. & Wood, J., 1994, Introduction to visualizing data validity. In: Hearnshaw, H.M. & Unwin, D.J. (Ed.s), *Visualisation in Geographical Information Systems*. John Wiley & Sons, Chichester, pp. 141-149.
- [22]. Hobrough, G. L., 1968, *Automation in Photogrammetric Instruments*, *Photogrammetric Engineering*, Vol. 31, No. 4.
- [23]. Irvin, B.J., Ventura, S.J. & Slater, B.K. 1995. Landform classification for soil-landscape studies. (Online) ESRI. Available: <http://www.esri.com>.

- [24]. Jain Kamal and Ravibabu, M.V., 2006, Identification of landslide Zonation using aster generated digital elevation model, *The Indian Journal of Institution Survey (IJS)* Vol: 60, No: 1, pp 58-61
- [25]. Kyriakidis, P.C., Shortridge, A.M. and Goodchild, M.F., 1999, Geostatistics for conflation and accuracy assessment of digital elevation models. *International Journal of Geographical Information Science*, 13(7), 677-707.
- [26]. Kumler, M.P., 1994. An intensive comparison of Triangulated Irregular Networks (TIN) and Digital Elevation Models (DEM). *Cartographica*, 31(2), pp 45.
- [27]. Lillesand, T.M. & Kiefer, R.W., 2000, *Remote Sensing and Image Interpretation*. 4th Ed. John Wiley & Sons, New York.
- [28]. Li, Z., 1991, Effects of checkpoints on the reliability of DTM accuracy estimates obtained from experimental tests. *Photogrammetric Engineering & Remote Sensing*, 57(10), 1333-1340.
- [29]. Li, Z., 1992, Variation of the accuracy of DTMs with sampling interval, the *Photogrammetry Records*, 14 (79) pp:113-128
- [30]. Li, Z., 1993a, Theoretical models of the accuracy of digital terrain models: an evaluation and some observations. *Photogrammetric Record*, 14(82), 651-659.
- [31]. Li, Z., 1993b, Mathematical models of the accuracy of digital terrain model surfaces linearly constructed from square gridded data. *Photogrammetric Record*, 14(82), 661-673.

- [32]. Lark, R.M., 1999. Soil-landform relationships at within-field scale: an investigation using continuous classification. *Geoderma* 92, 141–165.
- [33]. L.C. Chen and J.Y. Rau, A unified solution for digital terrain model and orthoimage generation from SPOT stereopairs, *IEEE Trans. Geoscience Remote Sens.*, 31(6), 1243–1252, 1993.
- [34]. Lee, J. and Stucky, D. 1998 'On applying viewshed analysis for determining least-cost paths on Digital Elevation Models', *International Journal of Geographical Information Science* 12, no. 8, 891-905.
- [35]. Madani, M., 1986, The InterMap Analytic: The Analytical Stereoplotting System From Intergraph: Proceeding ISPRS Commission V, Ottawa, Canada
- [36]. Madani, M., 1991, Intergraph ImageStation Photogrammetric System, ISPRS Commission II/VII International Workshop – 3D in Remote Sensing and GIS: Systems and Applications, Munich, Germany, September
- [37]. Madani, M. (1996). Digital Aerial Triangulation - The Operational Performance," Presented at the XVIII ISPRS Congress, Vienna, Austria, July 9-19, 1996
- [38]. MacMillan, R.A. & Pettapiece, W.W. 1997. Soil-landscape models: Automated landform characterization and generation of soil-landscape models. Technical Bulletin No. 1997- 1 E, Research Branch, Agriculture and Agri-Food Canada,
- [39]. Moore, I.D., Gessler, P.E., Nielsen, G.A., Peterson, G.A., 1993. Soil attribute prediction using terrain analysis. *Soil Sci. Soc. Am. J.* 57, 443–452.



- [40]. O'Callaghan, J. F. and D. M. Mark, 1984, "The Extraction of Drainage Networks From Digital Elevation Data," *Computer Vision, Graphics and Image Processing*, 28: 328-344.
- [41]. O. Hofmann, H. Ebner, and P. Nave, DPS - A digital photogrammetric system for producing digital elevation models and orthophotos by means of linear-array scanner imagery, *Photogram. Eng. Remote Sens.*, 50, 1135-1142, 1984.
- [42]. O'Loughlin, E. M. 1986, Prediction of surface saturation zones in natural catchments by topographic analysis. *Water Resour. Res.* 22:794–804.
- [43]. Pennock, D.J., Zebarth, B.J., & De Jong E. 1987. Landform classification and soil distribution in hummocky terrain, Saskatchewan, Canada. *Geoderma*, 40,297-315
- [44]. Q. Zheng, V. Klemas, X.H. Yan, Z. Wang, and K.Kagleder, Digital orthorectification of space shuttle coastal ocean photographs. *Int. J. Remote Sens.*, 18(1), 197-211, 1997.
- [45]. Ravibabu, M.V. and Jain Kamal, 2005, "DEM Accuracy Aspects" proceedings 25th ISRS annual convention and national symposium, during December 6-9th.